

Spatio-temporal statistics (MATH4341)

Michaelmas term

‘Spatial statistics’

Georgios P. Karagiannis

georgios.karagiannis@durham.ac.uk

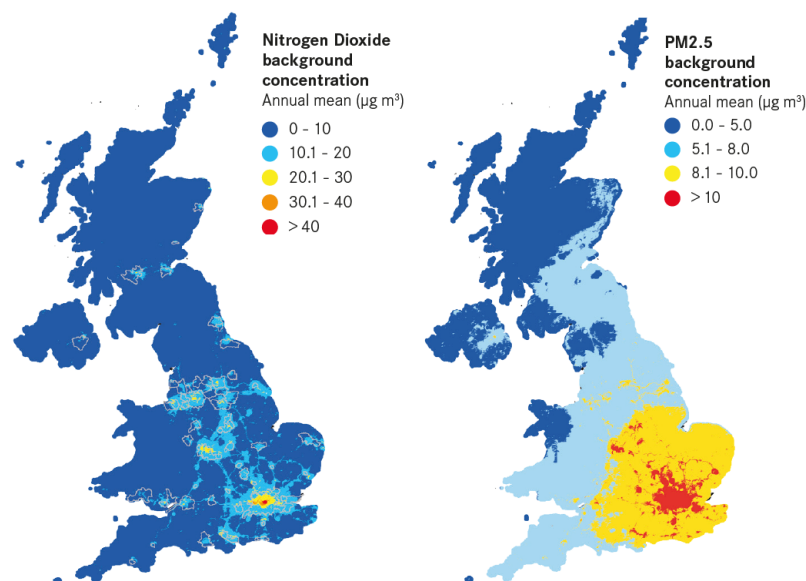
Department of Mathematical Sciences (Office MCS3088)
Durham University
Stockton Road Durham DH1 3LE UK

2024/10/30 at 13:33:02

Concepts

An introduction to spatial statistics:

- Regionalised statistical concepts
- Point referenced data analysis
- Aerial unit data analysis
- Point pattern data analysis
- Implementation in R



Lecture notes

1. Lecture notes part 1: Types of spatial data and modelling
2. Lecture notes part 2: Point referenced data modeling / Geostatistics
3. Lecture notes part 3: Aerial unit data / spatial data on lattices
4. Lecture notes part 4: Spatial point pattern modeling

Reading list

These lecture Handouts have been derived based on the above reading list.

Main textbooks (methods, implementation, and theory):

- Cressie, N. (2015). Statistics for spatial data. John Wiley & Sons.
- Kent, J. T., & Mardia, K. V. (2022). Spatial analysis (Vol. 72). John Wiley & Sons.
- Gaetan, C., & Guyon, X. (2010). Spatial statistics and modeling (Vol. 90). New York: Springer.
- Moller, J., & Waagepetersen, R. P. (2003). Statistical inference and simulation for spatial point processes. CRC press.

Main textbooks (software):

- Bivand, R. S., Pebesma, E. J., Gómez-Rubio, V., & Pebesma, E. J. (2008). Applied spatial data analysis with R (Vol. 747248717, pp. 237-268). New York: Springer.
- Moraga, P. (2023). Spatial statistics for data science: theory and practice with R. CRC Press.

Supplementary textbooks (methods, implementation, and theory):

- Banerjee, S., Carlin, B. P., & Gelfand, A. E. (2014). Hierarchical modeling and analysis for spatial data. CRC press.
- Ripley, B. D. (2005). Spatial statistics. John Wiley & Sons.
- Schabenberger, O., & Gotway, C. A. (2005). Statistical methods for spatial data analysis. CRC press
- Wackernagel, H. (2003). Multivariate geostatistics: an introduction with applications. Springer Science & Business Media.
- Diggle, P. J. (2013). Statistical analysis of spatial and spatio-temporal point patterns. CRC press.
- van Lieshout, M. N. M. (2019). Theory of spatial statistics: a concise introduction. CRC Press.

Lecture notes part 1: Types of spatial data

Lecturer & author: Georgios P. Karagiannis

georgios.karagiannis@durham.ac.uk

Aim. To introduce the types of spatial statistical data. To get a general idea about spatial statistics modeling.

Reading list & references:

- Cressie, N. (2015). Statistics for spatial data. John Wiley & Sons.
– Chapter 1: pp 1- 28

1. MOTIVATIONS

Note 1. Researchers in diverse areas such as geology, soil science, image processing, epidemiology, crop science, ecology, forestry, astronomy, atmospheric science, climatology, ecology, environmental health, and real estate marketing are increasingly faced with the task of analyzing data that are geographically referenced, and often presented as maps.

Note 2. In several problems, the data have a space (and time) label associated with them; this gives the motivation for the development and analysis of (not necessarily statistical) models that indicate whether there is dependence between measurements at different locations.

Note 3. In an epidemiological investigation, for instance, one might wish to analyze lung, breast, colorectal, and cervical cancer rates by county and year in a particular state, with smoking, mammography, and other important screening and staging information also available at some level. Public health professionals who collect such data are charged not only with surveillance, but also statistical inference tasks, such as modeling of trends and correlation structures, estimation of underlying model parameters, hypothesis testing (or comparison of competing models), and prediction of observations at unobserved locations (and times).

Note 4. Spatial statistics is the branch of statistics that focuses on the analysis and modeling of data with inherent spatial relationships, by accounting for spatial dependencies and patterns to derive meaningful insights and make informed decisions.

Shall I ignore spatial dependence? –No!

Note 5. Galton's problem (1888) arises in spatial statistics and cross-cultural research when observations are not statistically independent due to external dependencies like borrowing or common descent. For example, if two neighboring cultures share similar traits, it might

be due to cultural borrowing rather than independent development. This autocorrelation can lead to misleading conclusions if not properly accounted.

Note 6. From your experimental design lectures, recall R. A. Fisher's principles of randomization, blocking and replication to neutralize (not remove) spatial dependence. In his agricultural studies, he noticed that "After choosing the area we usually have no guidance beyond the widely verified fact that patches in close proximity are commonly more alike, as judged by the yield of crops, than those which are further apart." To avoid the "confounding" of treatment effect Fisher properly introduced randomization, namely the controlled introduction of uncertainty.

Note 7. The First Law of Geography, according to Waldo Tobler, is "*everything is related to everything else, but near things are more related than distant things.*" Perhaps, we can paraphrase it by using stats terms to "nearby attribute values are more statistically dependent than distant attribute values".

Example 8. ¹Consider a random sample $\{Z_i \in \mathbb{R}; i = 1, \dots, n\}$ jointly following a Normal distribution with unknown $E(Z_i) = \mu$ and known $\text{Var}(Z_i) = \sigma^2$.

Iid assumption: Assumption that the observables $\{Z_i\}$ are independent. This is equivalent to iid model $Z_i = \mu + \epsilon_i$ with $\epsilon_i \stackrel{\text{iid}}{\sim} N(0, \sigma^2)$.

AR assumption: Assumption that the observables $\{Z_i\}$ are positively autocorrelated as $\text{Cov}(Z_i, Z_j) = \sigma^2 \rho^{|i-j|}$ with known $\rho \in (0, 1)$. This is equivalent to AR model $Z_i = \rho Z_{i-1} + \epsilon_i$ with $\epsilon_i \stackrel{\text{iid}}{\sim} N(0, \sigma^2(1 - \rho^2))$.

Consider the case that the observables $\{Z_i\}$ are positively autocorrelated. Assume You fail to realize the presence of positive correlation in the data and You use the i.i.d model instead.

(1) Effect on parametric estimation of μ

The BLUE of μ is

$$(1.1) \quad \hat{Z} = \bar{Z} = \frac{1}{n} \sum_{i=1}^n Z_i$$

¹No need to worry how the equations are produced.

If the observables were iid then $\text{Var}(\hat{Z}|\text{iid obs}) = \frac{\sigma^2}{n}$. Since the observables are positively autocorrelated

$$(1.2) \quad \begin{aligned} \text{Var}(\hat{Z}|\text{AR obs}) &= \frac{1}{n} \sum_{i=1}^n \sum_{j=1}^n \text{Cov}(Z_i, Z_j) \\ &= \frac{\sigma^2}{n} \overbrace{\left(1 + 2 \frac{\rho}{1-\rho} \left(1 - \frac{1}{n} \right) - \frac{2}{n} \left(\frac{\rho}{1-\rho} \right)^2 \frac{1-\rho^{n-1}}{2} \right)}^{\tau_{n,\rho}=} \end{aligned}$$

If $n = 10$, and $\rho = 0.26$, the $1 - \alpha = 95\%$ confidence interval for μ is

$$\left\{ \bar{Z} \pm q_{\frac{\alpha}{2}} \sqrt{\text{Var}(\hat{Z}|\text{assump.})} \right\} \Rightarrow \begin{cases} \bar{Z} \pm \underbrace{1.96}_{q_{0.95}/2} \frac{\sigma}{\sqrt{10}} & \text{in i.i.d assum.} \\ \bar{Z} \pm \underbrace{2.485}_{=q_{0.95}/\sqrt{10,0.26}} \frac{\sigma}{\sqrt{10}} & \text{in AR assum.} \end{cases}$$

as $\sqrt{\tau_{10,0.26}} = 1.608$. Hence, if we fail to realize the presence of positive autocorrelation in the observables and wrongly the i.i.d model, the resulted confidence interval would be too narrow since the actual coverage probability is $\Phi(2.485) - \Phi(-2.485) = 87.5\%$ instead of 95%.

By re-writing the variance (1.2) as $\text{Var}(\hat{Z}) = \frac{\sigma^2}{n'}$ with

$$n' = n \left/ \left(1 + 2 \frac{\rho}{1-\rho} \left(1 - \frac{1}{n} \right) - \frac{2}{n} \left(\frac{\rho}{1-\rho} \right)^2 \frac{1-\rho^{n-1}}{2} \right) \right.,$$

we intuitively understand that the effect of the positive spatial correlation is that the equivalent independent observations in the above dataset with size n is n' (i.e. $n' \approx n \frac{1-\rho}{1+\rho}$, for large n). If $n = 10$, and $\rho = 0.26$, then $n' = 6.2$.

(2) Effect on predictive estimation of Z_{n+1}

Under the i.i.d. model, the predictor minimizing the MSPE for the next outcome Z_{n+1} is $\hat{Z}_{n+1}^{\text{iid}} = \bar{Z}$ and has

$$\text{MSPE}(\hat{Z}_{n+1}^{\text{iid}}|\text{dep obs}) = \sigma^2 \left(1 + 2 \frac{\rho}{1-\rho} \left(\rho^n - \frac{1}{n} \right) - 2 \left(\frac{\rho}{1-\rho} \right)^2 \frac{1-\rho^{n-1}}{2} \right)$$

Under the AR model the predictor minimizing the mse of the next outcome Z_{n+1} is

$$\hat{Z}_{n+1}^{\text{AR}} = \rho Z_n + (1-\rho) \frac{Z_1 + (1-\rho) \sum_{i=2}^{n-1} Z_i + Z_n}{n - (n-2)\rho}$$

with MSPE

$$\text{MSPE} \left(\hat{Z}_{n+1}^{\text{AR}} | \text{dep obs} \right) = \sigma^2 \left(1 - \rho^2 \frac{(1 + \rho)(1 - \rho)^2}{n - (n - 2)\rho} \right)$$

Note that the relative efficiency of this mistake is not too bad, e.g. for $n = 10$ and $\rho = 0.26$

$$\text{RE} = \frac{\text{MSPE} \left(\hat{Z}_{10+1}^{\text{AR}} | \text{dep obs} \right)}{\text{MSPE} \left(\hat{Z}_{10+1}^{\text{iid}} | \text{ind obs} \right)} = \frac{1.01952}{1.1} \approx 1.$$

However, if I consider large datasize $n \rightarrow \infty$ the asymptotic relative efficiency is

$$\text{ARE} = \lim_{n \rightarrow \infty} \frac{\text{MSPE} \left(\hat{Z}_{n+1}^{\text{AR}} | \text{dep obs} \right)}{\text{MSPE} \left(\hat{Z}_{n+1}^{\text{iid}} | \text{ind obs} \right)} = \dots = 1 - \rho^2 \approx \begin{cases} 93\% & , \rho = 0.26 \\ 75\% & , \rho = 0.5 \end{cases}$$

Spatial data and spatial process.

Note 9. In spatial statistics, the basic components are data $\{Z_1, \dots, Z_n\}$ observed at spatial locations $\{s_1, \dots, s_n\}$ correspondingly. Classically, the locations are 2D, $s \in S \subset \mathbb{R}^2$, however it can be $S \subset \mathbb{R}^1$ (such as in chromatography applications), or $S \subset \mathbb{R}^3$ (such as in earth science, 3D imaging, etc) depending on the application.

Note 10. Even more exotically, the spatial domain S does not necessarily need to be a Euclidean space (which our course will focus) such as $S \subset \mathbb{R}^d$, $d = 1, 2, 3, \dots$ but any topological space, eg sphere (recall Earth is round...).

Note 11. The locations $s_i \in S$ can be considered either (i.) fixed and hence used for training or (ii.) uncertain/random and hence a quantity for inference. Yet, $\{s_i\}$ can be arranged irregularly in the space or regularly in a grid. Data $Z_i = Z(s_i)$ are random vectors.

Note 12. Let $s \in \mathbb{R}^d$ be a generic data location, and suppose the datum $Z(s)$ at spatial location s is an uncertain and hence random vector. Considering s to vary over index set $S \subset \mathbb{R}^d$ imposes a spatial random field (or multivariate random process)

$$\{Z(s); s \in S\}$$

which can be modeled as a random field / random function / stochastic process (to be defined later.).

Note 13. In spatial problems, spatial data $\{Z_{s_i}\}_{i=1}^n$ at locations $\{s_i\}_{i=1}^n$ are assumed to be realizations of a random field (or a stochastic processes)

$$(1.3) \quad \{Z(s); s \in S\},$$

indexed by a spatial set $S \subset \mathbb{R}^d$.

2. PRINCIPAL SPATIAL STATISTICS AREAS

Note 14. We can characterize the spatial statistical problems according to the type of measurement, their specified (assumed) stochastic generating mechanism, and the choice of the spatial locations. In principle, each of them is associated to different motivations, statistical/scientific problems, statistical tools, however, modern applications/problems may involve characteristics from any combination of them.

Note 15. Here, we will study three of spatial statistical areas corresponding to point referenced data, aerial unit data, and point patterns.

2.1. Point referenced data / Geostatistics.

Note 16. Climate or environmental data are often presented in the form of a map, for example the maximum temperatures on a given day in a country, the concentrations of some pollutant in a city or the mineral content in soil. In mathematical terms, such maps can be described as realizations of a random function (random field/stochastic process); that is, an ensemble of random quantities indexed by points in a region of interest. The aim is usually interpolation, and the associated statistical inference.

Note 17. Such data were first analyzed in geological sciences. Hence, for historical reasons, this area of spatial statistics is often called Geostatistics and the point referenced data are also called geocoded or geostatistical data.

Note 18. Mathematically speaking, the spatial domain S is a continuous fixed subset of \mathbb{R}^d that contains a d -dimensional rectangle of positive volume. The datum $Z(s)$ is a random vector (outcome) at specific location $s \in S$ which can vary continuously over domain S . In practice, the actual data are observations $\{Z_i\}_{i=1}^n$ at n (finite number) fixed locations $\{s_i\}_{i=1}^n \subset S$ such as $Z_i = Z(s_i)$. The locations $\{s_i\}$ are fixed and can be arranged irregularly in the space or regularly as a grid.

Note 19. Geostatistics aims to answer questions about modeling, identification and separation of small and large scale variations, prediction at unobserved locations and reconstruction of the spatial process $Z(\cdot)$ across the whole space S .

Example 20. (Meuse river data set) Due to pollution of the Meuse river over many years, considerable amounts of heavy metals have accumulated in the overbank sediments of the embanked floodplains of their lower river reaches. The spatial variability of metal pollution of floodplain soils, which is controlled primarily by deposition of contaminated overbank sediments during flood events is under consideration. The process governing heavy metal distribution seems that polluted sediment is carried by the river, and mostly deposited close to the river bank, and areas with low elevation.

The Meuse river R dataset `meuse{sp}` contains locations and topsoil heavy metal concentrations (such as zinc, lead, copper, and cadmium), along with a number of soil and landscape variables at the observation locations, collected in a flood plain of the river Meuse, near the village of Stein (NL). Figure 2.1 shows 155 measurements of topsoil concentrations of the above heavy metals cadmium, copper, lead, and zinc collected in a flood plain of the river Meuse. Here, the locations $\{s_i\}$ are fixed and arranged irregularly as chosen by experimental design. The quantities of interest (QoI) $\{(Z_i^{\text{zinc}}, Z_i^{\text{lead}}, Z_i^{\text{cooper}}, Z_i^{\text{carmium}})\}$ are the concentrations of zinc, lead, copper, and cadmium, at these locations. Interest lie in prediction of QoI at unobserved locations (i.e. interpolation), quantification of the joint distribution of the QoI (evaluate the distribution of a random function $Z(s) = (Z^{\text{zinc}}(s), Z^{\text{lead}}(s), Z^{\text{cooper}}(s), Z^{\text{carmium}}(s))$, for all $s \in S$), and how each of QoI depends each other along the flood plain of the river Meuse is of interest (Figure 2.1f). If You ignore spatial dependency and implement standard multivariate statistical techniques (e.g. Fig 2.1e) to analyze the dependency of the QoI's you may obtain misleading results due to confounding space.

Example 21. (Coal ash dataset in Pennsylvania) Figure 2.2 shows 208 coal ash core measurements/samples collected on a regular grid of points in the Robena Mine in Greene County, Pennsylvania. The percentage of coal ash at the sampled locations is denoted by the colorbar. The sampled locations $\{s_i\}$ are fixed, and regularly spaced in a grid. As s are coordinates, they vary continuously over the spatial domain which is Robena Mine. The quantity of interest is the percentage of ash coal at these locations $\{Z(s_i)\}$. A mining engineer could be interested in predicting the ash distributions and the washability characteristics of coal along a seam in advance of mining. A spatial statistician would be able to produce a statistical model to predict ash concentrations between sampled points as well as quantify related uncertainties. Once a reasonable model that accounts for both the global trends and the local dependencies in the data is found and validated, the mining engineer could proceed to try and fill in the gaps, in other words, to estimate the percentage of coal ash at missing grid points based on the sampled percentages.

2.2. Aerial unit data / spatial data on lattices.

Note 22. Sometimes observations are collected over areal units such as pixels, census districts, or tomographic bins. In such cases, the random field models $\{Z(s); s \in S\}$ have a discrete index set S . The aims are usually, noise removal from an image and smoothing rather than interpolation.

Note 23. Mathematically speaking, the index set S of the data $\{Z(s)\}$ is a fixed (not random) and finite collection of points (locations) $s \in S$. The locations $s \in S$ can be irregular or arranged in a regular grid. Often, there is a natural adjacency relation or neighborhood

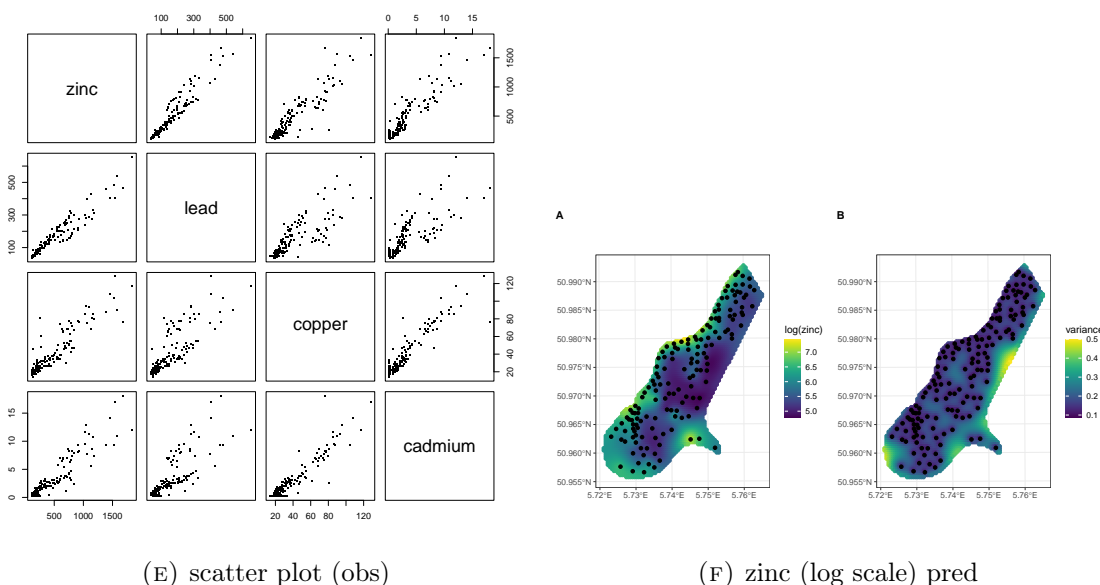


FIGURE 2.1. Map of the meuse dataset



FIGURE 2.2. (Coal ash data set) Percentage of coal ash at 208 locations.

structure. Often, datum $Z(s)$ is a random vector at location $s \in S$ and it represents an integral or average of the quantity of interest over some region represented by $s \in S$.

Example 24. In a UK epidemiological study, S may be the centroids of the UK counties, and $Z(s)$ may represent the average value of a characteristic in county s . In image processing, S may be a grid of pixels (locations are fixed and regular). In statistical physics, S may be a collection of atoms and genuinely finite (locations are fixed and regular).

Example 25. (Image restoration data) Figure 2.3a shows an (observed) image from a gray-scale photo-micrograph of the micro-structure of the Ferrite-Pearlite steel obtained by PNNL's project supported by DoE. The lighter part is ferrite while the darker part is pearlite. We focus our analysis on the first quarter fragment of size 240×320 pixels (red frame). This image is contaminated by noise due to the instrument errors. Interest lies in removing the noise (denoising) and recovering the real image. Figure 2.3b shows the restored image after appropriate statistical processing. Here the locations are pixels arranged in a fixed regular grid (hence discrete and not continuous). The each observation $Z(s)$ is the color of a pixel s ; here it is scalar as the observed pixels are in tones of grey, however it could be a 3D if the pixels were colored.

Example 26. (North Carolina SIDS data set) Figure 2.4a shows the total number of deaths from Sudden Infant Death Syndrome (SIDS) in 1974 for each of the 100 counties in North Carolina. Figure 2.4b shows the corresponding live births in each county and same period. This is the R data set `nc{spdep}`. The centroids of the counties do not lie on a regular grid. The sizes and shapes of the counties vary and can be quite irregular. The recorded counts are not tied to a precise location but tallied up county-wise. This kind of accumulation over administrative units is usual for privacy-sensitive data in, for instance, the crime or public health domains. A public health official could be interested in spatial patterns; e.g., whether

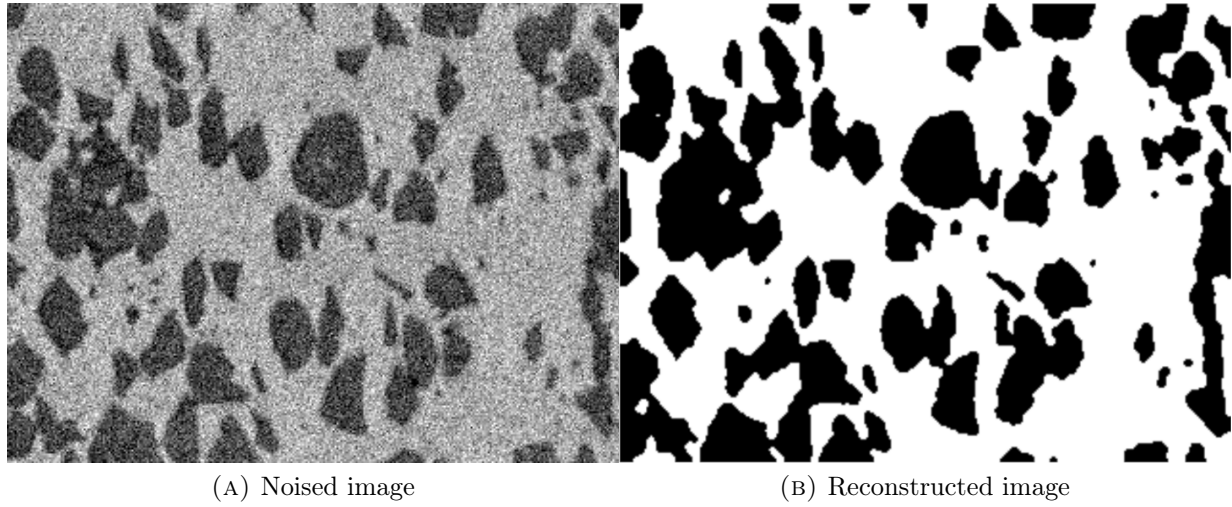


FIGURE 2.3. Ferrite-Pearlite steel image (Image restoration)

or not there are clusters of counties with a high incidence of SIDS, or areas where the SIDS counts are higher than what would be expected based on the number of live births in the area. Perhaps, we can eyeball the figures and see that there is a higher SIDS rate in the north-east areas compared to the north-west with similar birth numbers. A statistician can develop a statistical model providing inference about such questions.

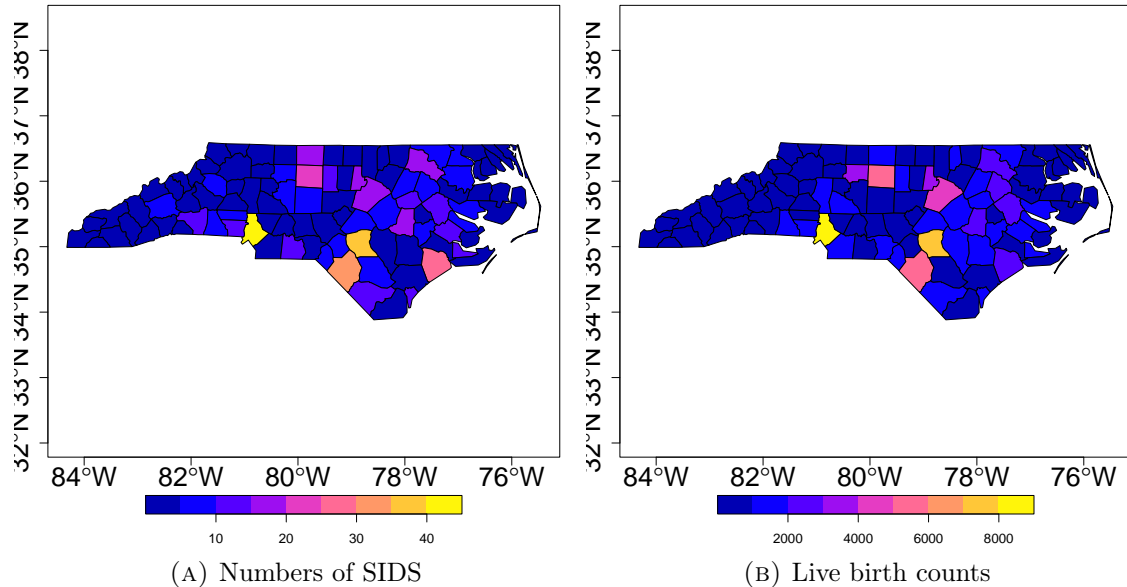


FIGURE 2.4. North Carolina SIDS data (Aerial unit data)

Example 27. (Columbus Columbus OH data set) Figures 2.5a, 2.5b, and 2.5c show the Property crime (number per thousand households) in 49 districts in Columbus in 1980, as
Page 9 Created on 2024/10/30 at 13:33:03 by Georgios Karagiannis

well as the average value of the house (in 1,000 USD), and the average household income (in 1,000 USD). This is the R dataset `columbus{spdep}`. The recorded counts are not tied to a precise household but tallied up county-wise (aerial unit) for privacy reasons. The locations $\{s_i\}$ are these areal unites; we observe they are not in a grid, and they do not have the same size or shape. Interest may lie to find whether high rates of crime are clustered in a particular areas, and if yes, perhaps what is the association of it with the value of the houses in the area.



FIGURE 2.5. Columbus Columbus OH spatial analysis dataset

2.3. Spatial point patterns.

Note 28. Sometimes the locations at which events occur are random. Typical examples include locations of trees in forests, outbreaks of forest fires, or epicentres of earthquakes. Such random patterns of locations are said to form a point pattern.

Note 29. Rigorously, the spatial domain S is a random set of points; specifically a point random field, in \mathbb{R}^d at which some events happened.

Note 30. In the simplest case, no covariate for Z is specified, and hence $Z(s)$ represents only the occurrences of an even at location s , one could think of the data taking scalar values $Z(s) = 1$ or $Z(s) = 0$ when the event has occurred or not for all $s \in S$. We will refer to it as a spatial point random field

Note 31. In the most general case, $Z(s)$ is a random vector at location $s \in S$ (eg other covariates are associated to the location s); these covariates are called marked variables. We will refer to it as a Marked spatial point random field.

Note 32. Questions in the spatial point pattern problems are mainly whether the pattern of locations is exhibiting complete spatial randomness, clustering (aggregation), or regularity (repulsiveness). In the marked spatial point random field where additional covariates are measured, we could possibly investigate the factors/variables associated to this behavior as well. A statistical approach to address such questions is needed as different observers may disagree on the amount of clustering or randomness. Usually patters from a completely random field may appear to be wrongly clustered when just eyeballed by an individual.

Example 33. (Tropical rain forest trees in Barro/Colorado) Figure 2.6 shows the positions (dots) of 3605 Beilschmiedia trees in a 1000×5000 meter rectangular stand in a tropical rain forest at Barro Colorado Island, Panama. All spatial coordinates are in the Cartesian coordinate system and in meters. Dataset is available from the R package `bei{spatstat}`. The scientific question may be if the trees are distributed over the area in a uniform way, they form clusters, or they are arrange in a specific pattern. Here, the locations of the dots/trees are not fixed but random/uncertain and of course they are matter of inference. This is a point random field as each location is associated to an occurrence only and not any other covariate. The statistician's task is to design models able to test and quantify heterogeneity/homogeneity.

Example 34. The domain scientist is interested in knowing whether the spatial locations are completely spatially random, clustered, or regularly distributed.

- (1) (Japanese pine trees) The Japanese pine trees dataset in R `japanesepines{spatstat}` represents locations of 65 saplings of Japanese black pine (*Pinus thunbergii*) in a 5.7×5.7 square meter sampling region in a natural forest.
- (2) (California Redwoods) The data represent the locations of 62 seedlings and saplings of California Giant Redwood (*Sequoiadendron giganteum*) recorded in a square sampling region.

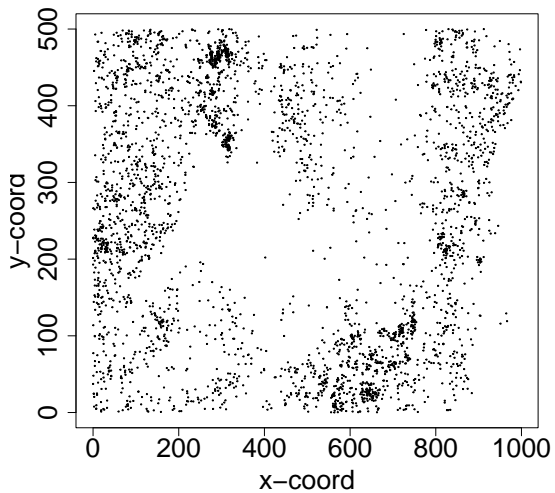


FIGURE 2.6. Locations of tropical rain forest trees in Barro/Colorado (Spatial point pattern data)

- (3) (Biological Cells) The data record the locations of the centres of 42 biological cells observed under optical microscopy in a histological section. The microscope field-of-view has been rescaled to the unit square.

Figure 2.7 presents the aforesaid spatial point patterns. It is difficult to eyeball, perhaps Figure 2.7a of the Japanese pine trees seems neither clustered nor regularly distributed but rather completely randomly distributed; Figure 2.7b of the California redwoods shows a clustered pattern; and Figure 2.7c shows a regular pattern.

Example 35. (Longleaf Pines Point Pattern) Figure 2.8 shows locations (as Cartesian coordinates) and relative diameters at breast height in dbh (as the size of the dot) of all longleaf pine trees in the 24ha region of the Wade Tract, an old-growth forest in Thomas County, Georgia in 1979. Dataset is available from R package `bei{spatstat}`. Longleaf pine is a fire-adapted species of trees. The domain scientist is interested in knowing whether the spatial locations are spatially random, or clustered, if large (small) trees cluster and how do large and small trees interact. A statistician can design models able to quantify such notions and provide inference. Here, the locations are random (not fixed) and in fact an object of inference. The diameter at breast height recorded along with the tree's location is the marked variable, and hence, the whole random field is a marked point random field.



FIGURE 2.7. Spatial Point Patterns

3. UNCERTAINTY QUANTIFICATION AND MODELING

Note 36. In spatial problems, uncertainty is expressed probabilistically through a spatial random field (or a stochastic process), which can be written most generally as

$$(3.1) \quad \{Y(s); s \in \mathcal{S}\},$$

To be
defined
rigorously
later



FIGURE 2.8. Longleaf Pines Point Pattern (Spatial point data)

Here $Y(s)$ is the random attribute value at location s , $\mathcal{S} \subset \mathbb{R}^d$ is a subset of \mathbb{R}^d ($d = 1, 2, 3$), contained in \mathcal{S} is a possibly random fixed or random set S that indexes those parts of \mathcal{S} relevant to the scientific study.

Spatial process model.

Note 37. The scientific uncertainty (i.e. the (known) uncertainty about the scientific problem) is expressed via the spatial process model. E.g., uncertainty about the real picture in Fig. 2.3a.

Note 38. This spatial random field can be a: geostatistical random field, lattice random field, or point random field depending on the principal spatial statistical area (Section 2) the application is associated with.

Note 39. The joint probability model defined by the random $\{Y(s); s \in S\}$ is

$$(3.2) \quad \text{pr}(Y, S) = \text{pr}(Y|S) \text{pr}(S)$$

Note 40. The specification of $\text{pr}(S)$ represents the three principal spatial statistical areas. E.g., for spatial data on lattices or point referenced data problems where the locations are fixed and not uncertain, we can consider $\text{pr}(Y, S) = \text{pr}(Y|S)$ with $\text{pr}(S) = 1_{\{S\}}(S)$ and hence ignore S and $\text{pr}(S)$ from the notation.

Data model.

Note 41. The measurement uncertainty is quantified via the data model. E.g. the “noisy image” in Fig. 2.3a.

Note 42. The data model is specified to be the conditional distribution of the data Z given the spatial random field Y and the S , namely

$$(3.3) \quad \text{pr}(Z|Y, S)$$

Note 43. If the data are assumed to be conditionally independent, such as $Z(s) \perp Z(s') | Y, S$ then

$$(3.4) \quad \text{pr}(Z|Y, S) = \prod_{i=1}^n \text{pr}(Z(s_i) | Y, S)$$

Note 44. The spatial statistical dependence of in Z , articulated by the First Law of Geography, follows by

$$\text{pr}(Z|S) = \int \text{pr}(Z|Y, S) \text{pr}(Y|S) dY$$

The hierarchical statistical model.

Note 45. To sum up the (known) uncertainty in spatial the statistics problem is expressed via the so called Hierarchical spatial model

$$(3.5) \quad \begin{cases} Z|Y, S & \text{data model} \\ Y, S & \text{spatial process model} \end{cases}$$

with

$$\text{pr}(Z, Y, S) = \text{pr}(Z|Y, S) \text{pr}(Y|S) \text{pr}(S)$$

Our interest it to learn $\text{pr}(Z^*|Z)$ or $\text{pr}(Y^*|Z)$ at any unseen locations s^* .

The Empirical (Bayes) hierarchical model.

Note 46. Often the decomposition (3.5) is parametrized with respect to unknown parameters $\theta \in \Theta$ we wish to learn given the observables; this is often called the Empirical hierarchical model i.e.

$$(3.6) \quad \begin{cases} Z|Y, S, \theta & \text{data model} \\ Y, S|\theta & \text{spatial process model} \end{cases}$$

with

$$\text{pr}(Z, Y, S|\theta) = \text{pr}(Z|Y, S, \theta) \text{pr}(Y|S, \theta) \text{pr}(S|\theta)$$

Our additional additional interest may be to learn the unknown θ via MLE

$$\hat{\theta} = \arg \min_{\theta} (\text{pr}(Z|\theta))$$

The Bayesian hierarchical model.

Note 47. In Bayesian statistics, the hierarchical model in (3.5) is completed by the $\theta \sim \text{pr}(\cdot)$ adding a third layer leading to the Bayesian hierarchical model

$$(3.7) \quad \begin{cases} Z|Y, S, \theta & \text{data model} \\ Y, S|\theta & \text{spatial process model} \\ \theta & \text{hyper-parameter prior model} \end{cases}$$

with

$$\text{pr}(Z, Y, S, \theta) = \text{pr}(Z|Y, S, \theta) \text{pr}(Y|S, \theta) \text{pr}(S|\theta) \text{pr}(\theta)$$

Our additional additional interest may be to learn the posterior of $\theta \text{pr}(\theta|Z)$.

Example 48. (A naive example: NOAA weather data) As dataset we consider a fraction from daily data originated from the US National Oceanic and Atmospheric Administration (NOAA) National Climatic Data Center and can be obtained from the IRI/LDEO Climate Data Library at Columbia University². The dataset is available from the R package in GitHub “andrewzm/STRbook”. In this example we focus on maximum temperature (Tmax) in degrees Fahrenheit ($^{\circ}\text{F}$) at 138 weather stations in the central USA (between 32°N - 46°N and 80°W - 100°W), recorded in 1st of May 1993. The data are not complete, in the sense that there are missing measurements at various stations and at various time points, and the stations themselves are obviously not located everywhere in the central USA. (Figure Figure 3.1)

This data set contains $n = 138$ observations $\{(Z_i, s_i)\}_{i=1}^n$ where the i -th observation contains the maximum temperature (Tmax) in degrees Fahrenheit ($^{\circ}\text{F}$) Z_i at location specified by coordinates $s_i = (s_{1,i}, s_{2,i})^{\top}$ that is the latitude degrees north of the Equator $s_{2,i}$, and longitude degrees west of Greenwich $s_{1,i}$. See Figure 3.1.

This is definitely a geostatistics problem. Here, we will present a naive way to model it by reflecting what we discussed earlier.

Data model: One may consider that the observations $\{Z_i\}$ at each location are the result of observing the real (hence unknown) maximum temperature Y_i but contaminated by “additive random noise” with unknown scale $\sigma > 0$ due to instrumental error, i.e.

$$Z_i = Y_i + \epsilon_i, \quad \epsilon_i \sim N(0, \sigma^2), \quad i = 1, \dots, n \implies Z_i|Y_i, \sigma^2 \stackrel{\text{ind}}{\sim} N(Y_i, \sigma^2), \quad i = 1, \dots, n$$

Spatial process model: One may consider that the real maximum temperature $Y(s)$ (over the spatial domain $s \in S$) is a function where at each finite set of locations $\{s_i\}_{i=1}^n$ follows a Normal distribution with a mean μ with $[\mu]_i = \mu(s_i)$ parameterized

That's a
snapshot
for what
follows.

²<http://iridl.ldeo.columbia.edu/SOURCES/.NOAA/.NCDC/.DAILY/.FSOD/>



FIGURE 3.1. NOAA weather data (1 May 1993)

as

$$\mu(s) = \beta_0 + \beta_1 s_1 + \beta_2 s_2 + \beta_{12} s_1 s_2, \text{ at a location } s = (s_1, s_2)^\top$$

with unknown parameter β , and covariance matrix $[C]_{i,j} = c(s_i, s_j)$ parameterized with covariance function

$$c(s, s') = \sigma^2 \exp(-\phi \|s - s'\|)$$

to impose that nearer locations cause stronger dependences in the model. Here β , ϕ , and σ^2 are unknown parameters.

Hierarchical model: To sum up, we have build the hierarchical model

$$(3.8) \quad \begin{cases} Z|Y, \sigma^2 \sim N_n(Y, I\sigma^2), & \text{data model} \\ Y|\sigma^2, \beta, \phi \sim N_n(S\beta, C), & \text{spatial process model} \end{cases}$$

Figure 3.2 shows the hierarchical spatial model (3.8) for different values of $\theta = (\sigma^2, \beta, \phi)$; the surface corresponds to the spatial process $\{Y(s); s \in \mathbb{R}^2\}$ and is presented at three different instances each of them with different values for (β, ϕ) , while the dots correspond to the observations $\{(Z(s_i), s_i)\}_{i=1}^n$ and their deviation from the spatial process is controlled by σ^2 . Note that marginally

$$Z|\sigma^2, \beta, \phi \sim N_n(S\beta, \sigma^2(I + C)).$$

Bayesian hierarchical model: If we work on the fully Bayesian framework, we can complete the model with priors on $\theta = (\sigma^2, \beta, \phi)$ for instance $\sigma^2 \sim IG(\kappa_\sigma, \lambda_\sigma)$, $\phi \sim$



FIGURE 3.2. Examples representing the hierarchical spatial model (3.8) for different values of $\theta = (\sigma^2, \beta, \phi)$

$\text{IG}(\kappa_\phi, \lambda_\phi)$, and $\beta \sim N_4(b, Iv)$, with some known hyper-parameters $\kappa_\sigma, \lambda_\sigma, \kappa_\phi, \lambda_\phi, b, v$. To sum up, we have build the Bayesian model

$$\left\{ \begin{array}{ll} Z|Y, \sigma^2 \sim & N_n(Y, I\sigma^2), \text{ data model} \\ Y|\sigma^2, \beta, \phi \sim & N_n(S\beta, C), \text{ spatial process model} \\ \beta \sim & N_4(b, Iv), \text{ hyper-parameter prior model} \\ \sigma^2 \sim & \text{IG}(\kappa_\sigma, \lambda_\sigma), \text{ hyper-parameter prior model} \\ \phi \sim & \text{IG}(\kappa_\phi, \lambda_\phi), \text{ hyper-parameter prior model} \end{array} \right.$$

4. SPATIO-TEMPORAL STATISTICS

Note 49. Spatio-temporal data arise when information is both spatially and temporally referenced. Any of the aforesaid spatial statistics cases can be extended and become temporal. Such methods will be discussed in the Epiphany term. This is where we aim at the end of the module.

Example 50. We extend the dataset in the Spatial statistics Example 48 by considering time.

The dataset is available from the R package in GitHub “andrewzm/STRbook”. These daily data originated from the US National Oceanic and Atmospheric Administration (NOAA) National Climatic Data Center and can be obtained from the IRI/LDEO Climate Data Library at Columbia University. The data set we consider consists the daily maximum temperature (Tmax) in degrees Fahrenheit ($^{\circ}\text{F}$) at weather stations in the central USA (between 32°N – 46°N and 80°W – 100°W), recorded between May-July in year 1993. These data are considered to be discrete and regular in time (daily) and geostatistical and irregular in space. However, the data are not complete, in that there are missing measurements at various stations and at various time points, and the stations themselves are obviously not located everywhere in the central USA. See Figure 4.1.

Interest lies on not only how the maximum temperature is only distributed over the spatial domain but also how it evolves during the time.

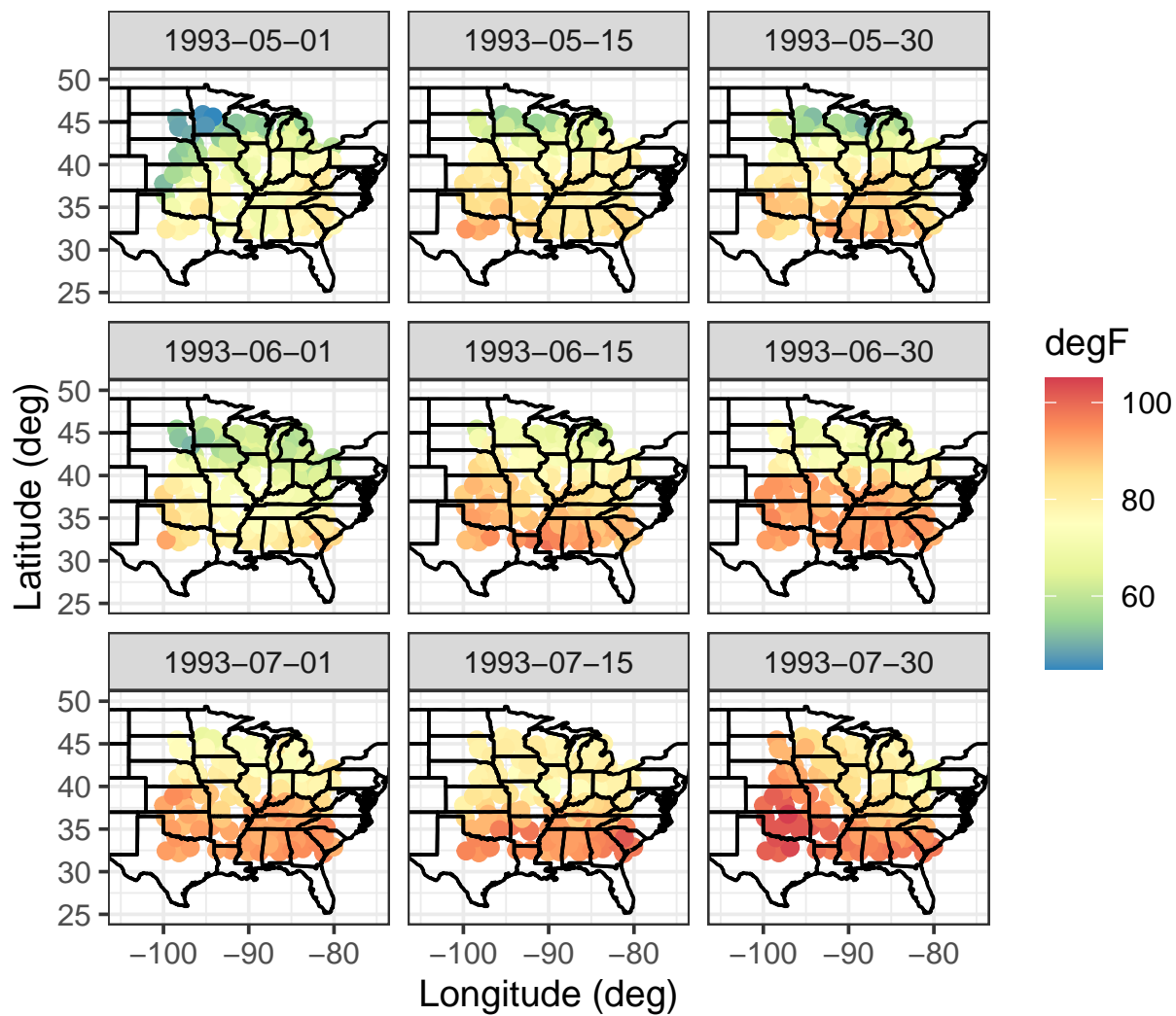


FIGURE 4.1. NOAA daily weather data

Lecture notes part 2: Point referenced data modeling / Geostatistics

Lecturer & author: Georgios P. Karagiannis

georgios.karagiannis@durham.ac.uk

Aim. To introduce point referenced data modeling (geostatistics) with particular focus on concepts spatial variables, random fields, semi-variogram, kriging, change of support, multivariate geostatistics, for Bayesian and classical inference.

Reading list & references:

- [1] Cressie, N. (2015; Part I). Statistics for spatial data. John Wiley & Sons.
- [2] Kent, J. T., & Mardia, K. V. (2022). Spatial analysis (Vol. 72). John Wiley & Sons.
- [3] Chiles, J. P., & Delfiner, P. (2012). Geostatistics: modeling spatial uncertainty (Vol. 713). John Wiley & Sons.
- [4] Wackernagel, H. (2003). Multivariate geostatistics: an introduction with applications. Springer Science & Business Media.
- [5] Gaetan, C., & Guyon, X. (2010; Ch 2 & 5.1). Spatial statistics and modeling (Vol. 90). New York: Springer.

Part 1. Basic stochastic models & related concepts for model building

Note 1. We discuss basic stochastic models and concepts for modeling point referenced data in the Geostatistics framework.

1. RANDOM FIELDS (OR STOCHASTIC PROCESSES)

Definition 2. A random field (or stochastic process, or random function) $Z = (Z(s); s \in \mathcal{S})$ taking values in $\mathcal{Z} \subseteq \mathbb{R}^q$, $q \geq 1$ is a family of random variables $\{Z(s) := Z(s; \omega); s \in \mathcal{S}, \omega \in \Omega\}$ defined on the same probability space $(\Omega, \mathfrak{F}, \text{pr})$ and taking values in \mathcal{Z} . The label $s \in \mathcal{S}$ is called site, the set $\mathcal{S} \subseteq \mathbb{R}^d$ is called the (spatial) set of sites at which the random field is defined, and \mathcal{Z} is called the state space of the field.

Note 3. Given a set of sites $\{s_1, \dots, s_n\}$, with $s_i \in \mathcal{S}$ and $n \in \mathbb{N}$, the random vector $(Z(s_1), \dots, Z(s_n))^\top$ has a well-defined probability distribution that is completely determined by its joint CDF

$$F_{s_1, \dots, s_n}(z_1, \dots, z_n) := \text{pr}(Z(s_1) \leq z_1, \dots, Z(s_n) \leq z_n)$$

The family of all finite-dimensional distributions (or fidi's) of Z is called the spatial distribution of the process .

Note 4. According to Kolmogorov Theorem 5, to define a random field model, one must specify the joint distribution of $(Z(s_1), \dots, Z(s_n))^\top$ for all of n and all $\{s_i \in S; i = 1, \dots, n\}$ in a consistent way.

Proposition 5. (*Kolmogorov consistency theorem*) Let pr_{s_1, \dots, s_n} be a probability on \mathbb{R}^n with join CDF F_{s_1, \dots, s_n} for every finite collection of points s_1, \dots, s_n . If F_{s_1, \dots, s_n} is symmetric w.r.t. any permutation \mathbf{p}

$$F_{\mathbf{p}(s_1), \dots, \mathbf{p}(s_n)}(z_{\mathbf{p}(1)}, \dots, z_{\mathbf{p}(n)}) = F_{s_1, \dots, s_n}(z_1, \dots, z_n)$$

for all $n \in \mathbb{N}$, $\{s_i \in S\}$, and $\{z \in \mathbb{R}\}$, and all if all permutations \mathbf{p} are consistent in the sense

$$\lim_{z_n \rightarrow \infty} F_{s_1, \dots, s_n}(z_1, \dots, z_n) = F_{s_1, \dots, s_{n-1}}(z_1, \dots, z_{n-1})$$

or all $n \in \mathbb{N}$, $\{s_i \in S\}$, and $\{z_i \in \mathbb{R}\}$, then there exists a random field Z whose fidi's coincide with those in F .

Example 6. Let $n \in \mathbb{N}$, let $\{X_i : \mathcal{S} \rightarrow \mathbb{R}; i = 1, \dots, n\}$ be a set of constant functions, and let $\{Z_i \sim N(0, 1)\}_{i=1}^n$ be a set of independent random variables. Then

$$(1.1) \quad \tilde{Z}(s) = \sum_{i=1}^n Z_i X_i(s), \quad s \in S$$

is a well defined random field as it satisfies Theorem 5.

1.1. Mean and covariance functions.

Definition 7. The mean function $\mu(\cdot)$ and covariance function $c(\cdot, \cdot)$ of a random field $(Z(s); s \in \mathcal{S})$ are defined as

$$(1.2) \quad \mu(s) = E(Z(s)), \quad \forall s \in \mathcal{S}$$

$$(1.3) \quad c(s, s') = \text{Cov}(Z(s), Z(s')) = E((Z(s) - \mu(s))(Z(s') - \mu(s'))^\top), \quad \forall s, s' \in \mathcal{S}$$

Example 8. For (1.1), the mean function is $\mu(s) = E(\tilde{Z}_s) = 0$ and covariance function is

$$\begin{aligned} c(s, s') &= \text{Cov}(Z(s), Z(s')) = \text{Cov}\left(\sum_{i=1}^n Z_i X_i(s), \sum_{j=1}^n Z_j X_j(s')\right) \\ &= \sum_{i=1}^n X_i(s) \sum_{j=1}^n X_j(s') \underbrace{\text{Cov}(Z_i, Z_j)}_{1(i=j)} = \sum_{i=1}^n X_i(s) X_i(s') \end{aligned}$$

1.1.1. Construction of covariance functions.

Note 9. What follows provides the means for checking and constructing covariance functions.

Proposition 10. The function $c : \mathcal{S} \times \mathcal{S} \rightarrow \mathbb{R}$, $\mathcal{S} \subseteq \mathbb{R}^d$ is a covariance function iff $c(\cdot, \cdot)$ is semi-positive definite; i.e.

$$\forall n \in \mathbb{N} - \{0\}, \forall (a_1, \dots, a_n) \in \mathbb{R}^n \text{ and } \forall (s_1, \dots, s_n) \in \mathcal{S}^n : \sum_{i=1}^n \sum_{j=1}^n a_i a_j c(s_i, s_j) \geq 0$$

or in other words, the Gram matrix $(c(s_i, s_j))_{i,j=1}^n$ is non-negative definite for any $\{s_i\}_{i=1}^n$, $n \in \mathbb{N} - \{0\}$.

Example 11. $c(s, s') = 1(\{s = s'\})$ is a proper covariance function because

$$\sum_i \sum_j a_i a_j c(s_i, s_j) = \sum_i a_i^2 \geq 0, \quad \forall a$$

Note 12. One way to construct a c.f c is to set $c(s, s') = \psi(s)^\top \psi(s')$, for a given vector of basis functions $\psi(\cdot) = (\psi_1(\cdot), \dots, \psi_n(\cdot))$.

Proof. From Proposition 10, as

$$\sum_i \sum_j a_i a_j c(s_i, s_j) = (\psi a)^\top (\psi a) \geq 0, \quad \forall a \in \mathbb{R}^n$$

□

2. SECOND ORDER RANDOM FIELDS (OR SECOND ORDER PROCESSES)

Note 13. We introduce a particular class of random fields whose mean and covariance functions exist and which can be used for spatial data modeling.

Definition 14. Second order random field (or second order process) $(Z(s); s \in \mathcal{S})$ is called the random field where $E((Z(s))^2) < \infty$ for all $s \in \mathcal{S}$.

Example 15. In second order random field $(Z(s); s \in \mathcal{S})$ the associated mean function $\mu(\cdot)$ and covariance function $c(\cdot, \cdot)$ exist, because $c(s, t) = E(Z(s)Z(t)) - E(Z(s))E(Z(t))$ for $s, t \in \mathcal{S}$.

3. GAUSSIAN RANDOM FIELD (OR GAUSSIAN PROCESS)

Note 16. Gaussian random field (GRF) is a particular class of second order random field which is widely used in spatial data modeling due to its computational tractability.

Also

Definition 17. $(Z(s); s \in \mathcal{S})$ is a Gaussian random field (GRF) or Gaussian process (GP) on \mathcal{S} if for any $n \in \mathbb{N}$ and for any finite set $\{s_1, \dots, s_n; s_i \in \mathcal{S}\}$, the random vector $(Z(s_1), \dots, Z(s_n))^\top$ follows a multivariate normal distribution.

Example Proposition

Proposition 18. A GP $(Z(s); s \in \mathcal{S})$ is fully characterized by its mean function $\mu : S \rightarrow \mathbb{R}$ with $\mu(s) = E(Z(s))$, and its covariance function with $c(s, s') = Cov(Z(s), Z(s'))$.

Note 19. Hence, we denote the GP as $Z(\cdot) \sim \mathcal{GP}(\mu(\cdot), c(\cdot, \cdot))$.

Note 20. When using GP for spatial modeling we just need to specify its functional parameters i.e. the mean and covariance functions.

Note 21. Popular forms of mean functions are polynomial expansions, such as $\mu(s) = \sum_{j=0}^{p-1} \beta_j s^j$ for tunable unknown parameter β . A popular form of covariance functions (c.f.), for tunable unknown parameters $\phi > 0$, and $\sigma^2 > 0$, are

- (1) Exponential c.f. $c(s, s') = \sigma^2 \exp(-\phi \|s - s'\|_1)$
- (2) Gaussian c.f. $c(s, s') = \sigma^2 \exp(-\phi \|s - s'\|_2^2)$
- (3) Nugget c.f. $c(s, s') = \sigma^2 \mathbf{1}(s = s')$

Example 22. Recall your linear regression lessons where you specified the sampling distribution to be $y_x | \beta, \sigma^2 \stackrel{\text{ind}}{\sim} N(x^\top \beta, \sigma^2)$, $\forall x \in \mathbb{R}^d$. Well that can be considered as a GP $Z(\cdot) \sim \mathcal{GP}(\mu(\cdot), c(\cdot, \cdot))$ with $\mu(x) = x^\top \beta$ and $c(x, x') = \sigma^2 \mathbf{1}(x = x')$ in (3).

Example 23. Figures 3.1 & 3.2 presents realizations of GRF $Z(\cdot) \sim \mathcal{GP}(\mu(\cdot), c(\cdot, \cdot))$ with $\mu(s) = 0$ and differently parameterized covariance functions in 1D and 2D. In 1D the code to simulate the GP is given in Algorithm 1. Note that we actually discretize it and simulate it from the fidi.

Algorithm 1 R script for simulating from a GP ($Z(s); s \in \mathbb{R}^1$) with $\mu(s) = 0$ and $c(s, t) = \sigma^2 \exp(-\phi \|s - t\|_2^2)$

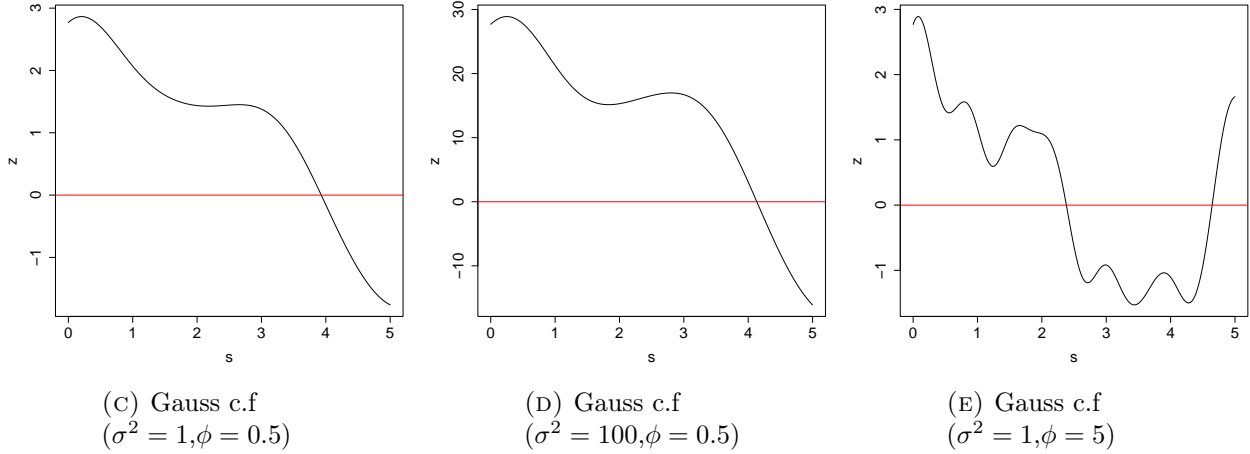
```
# set the GP parameterized mean and covariance function
mu_fun <- function(s) { return (0) }
cov_fun_gauss <- function(s,t,sig2,phi) {
    return ( sig2*exp(-phi*norm(c(s-t),type="2")**2) )
}
# discretize the problem in n = 100 spatial points
n <- 100
s_vec <- seq(from = 0, to = 5, length = n)
mu_vec <- matrix(nrow = n, ncol = 1)
Cov_mat <- matrix(nrow = n, ncol = n)
# compute the associated mean vector and covariance matrix of the n=100 dimensional
# Normal r.v.
sig2_val <- 1.0 ;
phi_val <- 5
for (i in 1:n) {
    mu_vec[i] <- mu_fun(s_vec[i])
    for (j in 1:n) {
        Cov_mat[i,j] <- cov_fun_gauss(s_vec[i],s_vec[j],sig2_val,phi_val)
    }
}
# simulate from the associated distribution
z_vec <- mu_vec + t(chol(Cov_mat))%*%rnorm(n, mean=0, sd=1)
# plot the path (R produces a line plot)
plot(s_vec, z_vec, type="l")
abline(h=0,col="red")
```

Nugget c.f. is the usual noise where the height of ups and downs are random and controlled by σ^2 (Figures 3.1a & 3.1b ; Figures 3.2a & 3.2b). In Gaussian c.f. the height of ups and downs are random and controlled by σ^2 (Fig.3.1c & 3.1d ; Figures 3.2c & 3.2d), and the spatial dependence / frequency of the ups and downs is controlled by β (Figures 3.1d & 3.1e ; Figures 3.2d & 3.2e). Realizations with different c.f. have different behavior (Figures 3.1a, 3.1d & 3.1e ; Figures 3.2a, 3.2d & 3.2e)



(A) Nugget c.f
 $(\sigma^2 = 1)$

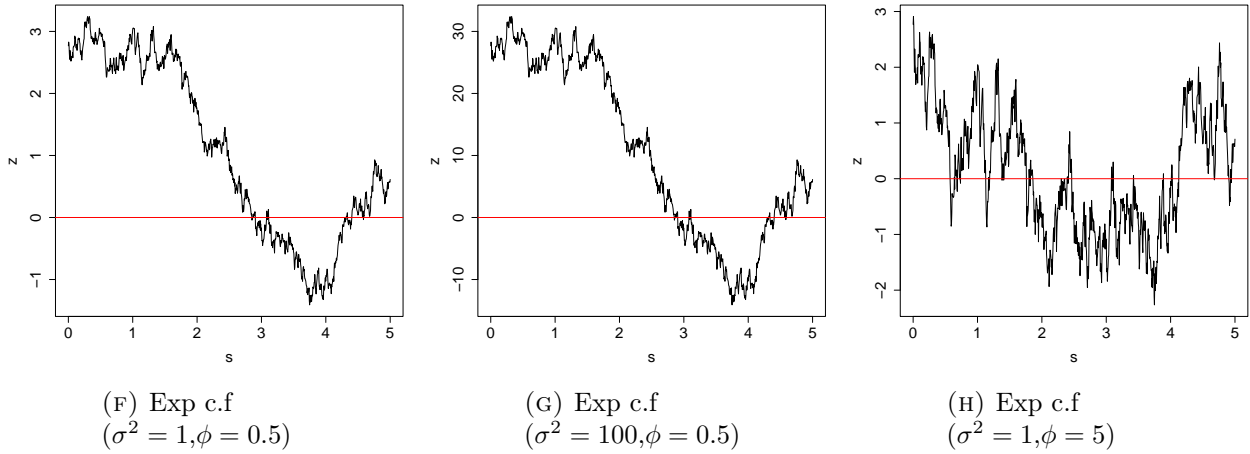
(B) Nugget c.f
 $(\sigma^2 = 100)$



(C) Gauss c.f
 $(\sigma^2 = 1, \phi = 0.5)$

(D) Gauss c.f
 $(\sigma^2 = 100, \phi = 0.5)$

(E) Gauss c.f
 $(\sigma^2 = 1, \phi = 5)$



(F) Exp c.f
 $(\sigma^2 = 1, \phi = 0.5)$

(G) Exp c.f
 $(\sigma^2 = 100, \phi = 0.5)$

(H) Exp c.f
 $(\sigma^2 = 1, \phi = 5)$

FIGURE 3.1. Realizations of GRF $Z(\cdot) \sim \mathcal{GP}(\mu(\cdot), c(\cdot, \cdot))$ when $s \in [0, 5]$ (using same seed)

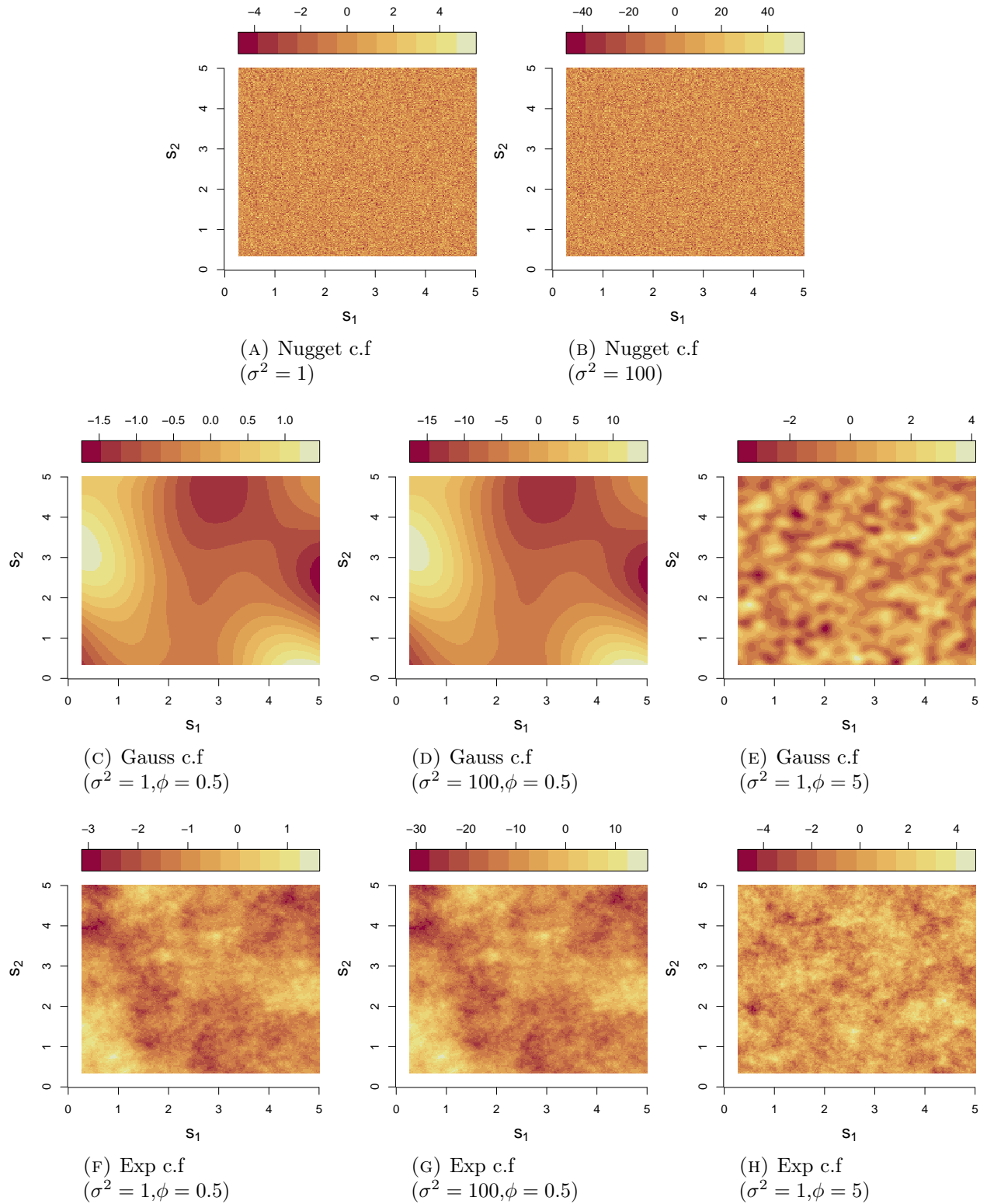


FIGURE 3.2. Realizations of GRF $Z(\cdot) \sim \mathcal{GP}(\mu(\cdot), c(\cdot, \cdot))$ when $s \in [0, 5]^2$ (using same seed)

4. STRONG STATIONARITY

Note 24. We introduce a specific behavior of random field to build our models.

Notation 25. Formally, we define the separation (or lag) set as $\mathcal{H} = \{h \in \mathbb{R}^d : s \in \mathcal{S}, s + h \in \mathcal{S}\}$ where $\mathcal{S} \subseteq \mathbb{R}^d$ is the spatial domain for $d = 1, 2, 3, \dots$. However, we will consider cases where $\mathcal{S} = \mathbb{R}^d$ and $\mathcal{H} = \mathbb{R}^d$ for $d = 1, 2, 3, \dots$ in Euclidean spaces.

Definition 26. A random field $(Z(s); s \in \mathcal{S})$ is strongly stationary on \mathcal{S} if for all finite sets consisting of $s_1, \dots, s_n \in \mathcal{S}$, $n \in \mathbb{N}$, for all $k_1, \dots, k_n \in \mathbb{R}$, and for all $h \in \mathcal{H}$

$$\text{pr}(Z(s_1 + h) \leq k_1, \dots, Z(s_n + h) \leq k_n) = \text{pr}(Z(s_1) \leq k_1, \dots, Z(s_n) \leq k_n)$$

Note 27. Yuh... strong stationary may represent a behavior being too “restrictive” to be used for spatial data modeling as it is able to represent only limiting number of spatial dependencies.

5. WEAK STATIONARITY (OR SECOND ORDER STATIONARITY)

Note 28. We introduce another weaker behavior of random field able to represent a larger class of spatial dependencies.

Note 29. Instead of working with the “restrictive” strong stationarity, we could just properly specify the behavior of the first two moments only; notice that Definition 26 implies that, given $E((Z(s))^2) < \infty$, it is $E(Z(s)) = E(Z(s + h)) = \text{const} \dots$ and $\text{Cov}(Z(s), Z(s')) = \text{Cov}(Z(s + h), Z(s' + h)) \stackrel{h=-s'}{\equiv} \text{Cov}(Z(s - s'), Z(0)) = \text{funct of lag} \dots$

Definition 30. A random field $(Z(s); s \in \mathcal{S})$ is called stationary random field (s.r.f.) (or weakly stationary or second order stationary) if it has constant mean and translation invariant covariance; i.e. for all $s, s' \in \mathbb{R}^d$,

- (1) $E((Z(s))^2) < \infty$ (finite)
- (2) $E(Z(s)) = \mu$ (constant)
- (3) $\text{Cov}(Z(s), Z(s')) = c(s' - s)$ for some even function $c : \mathcal{S} \rightarrow \mathbb{R}$ (lag dependency)

Definition 31. Stationary (or weakly or second order stationary) covariance function is called the c.f. of a stationary random field.

6. COVARIOGRAM

Note 32. We introduce the covariogram function able to express many aspects of the behavior of a (weakly) stationary random field and hence be used as statistical descriptive tool.

Definition 33. The covariogram function of a weakly stationary random field $(Z(s); s \in \mathcal{S})$ is defined by $c : \mathcal{H} \rightarrow \mathbb{R}$ with

$$c(h) = \text{Cov}(Z(s), Z(s+h)), \forall s \in \mathcal{S}, \forall h \in \mathcal{H}.$$

Example 34. For the Gaussian c.f. $c(s, t) = \sigma^2 \exp(-\phi \|s - t\|_2^2)$ in (Ex. 20(2)), we may denote just

$$(6.1) \quad c(h) = c(s, s+h) = \sigma^2 \exp(-\phi \|h\|_2^2)$$

Observe that, in Figures 3.1 & 3.2, the smaller the ϕ , the smoother the realization (aka slower changes). One way to justify this observation is to think that smaller values of ϕ essentially bring the points closer by re-scaling spatial lags h in the c.f.

Proposition 35. If $c : \mathcal{H} \rightarrow \mathbb{R}$ is the covariogram of a weakly stationary random field $(Z(s); s \in \mathcal{S})$ then:

- (1) $c(h) = c(-h)$ for all $h \in \mathcal{H}$
- (2) $|c(h)| \leq c(0) = \text{Var}(Z(s))$ for all $h \in \mathcal{H}$
- (3) $c(\cdot)$ is semi-positive definite; i.e. for all $n \in \mathbb{N} - \{0\}$, $(a_1, \dots, a_n) \in \mathbb{R}^n$, and $(s_1, \dots, s_n) \subseteq \mathcal{S}^n$

$$\sum_{i=1}^n \sum_{j=1}^n a_i a_j c(s_i - s_j) \geq 0$$

Note 36. Given there is some knowledge of the characteristic functions of a suitable distribution, the following spectral representation theorem helps in the specification of a suitable covariogram.

Theorem 37. (Bochner's theorem) Let $c : \mathbb{R}^d \rightarrow \mathbb{R}$ be a continuous even real-valued function for $d \geq 1$. Then $c(\cdot)$ is positive semidefinite (hence a covariogram of a stationary random field) if and only if it can be represented as

$$c(h) = \int_{\mathbb{R}^d} \exp(i\omega^\top h) dF(\omega)$$

where F is a symmetric positive finite measure on \mathbb{R}^d called spectral measure.

Note 38. In our course, we focus on cases where F has a density $f(\cdot)$ i.e. $dF(\omega) = f(\omega) d\omega$. $f(\cdot)$ is called spectral density of $c(\cdot)$, it is

$$c(h) = \int_{\mathbb{R}^d} \exp(i\omega^\top h) f(\omega) d\omega,$$

and it dies as $\lim_{|h| \rightarrow \infty} c(h) = 0$

Theorem 39. If $c(\cdot)$ is integrable, the spectral density $f(\cdot)$ can be computed by inverse Fast Fourier transformation

$$f(\omega) = \left(\frac{1}{2\pi}\right)^d \int_{\mathbb{R}^d} \exp(-i\omega^\top h) c(h) dh$$

Example 40. Consider the Gaussian c.f. $c(h) = \sigma^2 \exp(-\phi \|h\|_2^2)$ for $\sigma^2, \phi > 0$ and $h \in \mathbb{R}^d$. Then, by using Theorem 37, the spectral density is

$$\begin{aligned} f(\omega) &= \left(\frac{1}{2\pi}\right)^d \int_{\mathbb{R}^d} \exp(-i\omega^\top h) \sigma^2 \exp(-\phi \|h\|_2^2) dh \\ &= \sigma^2 \left(\frac{1}{2\pi}\right)^d \prod_{j=1}^d \int_{\mathbb{R}} \exp(-i\omega_j h_j - \phi h_j^2) dh_j \\ &= \sigma^2 \left(\frac{1}{2\pi}\right)^d \prod_{j=1}^d \int_{\mathbb{R}} \exp(-\phi(h_j - (-i\omega/(2\phi)))^2) \exp(-\omega_j^2/(4\phi)) dh_j \\ &= \sigma^2 \left(\frac{1}{4\pi\phi}\right)^{d/2} \exp(-\|\omega\|_2^2/(4\phi)) \end{aligned}$$

i.e. it has a Gaussian form.

Definition 41. Let $(Z(s) : s \in \mathcal{S})$ be a weakly stationary random field with covariogram function $c : \mathcal{H} \rightarrow \mathbb{R}$ and $c(h) = \text{Cov}(Z(s), Z(s+h))$. The correlogram function $\rho : \mathcal{H} \rightarrow [-1, 1]$ is defined as

$$\rho(h) = \frac{c(h)}{c(0)}.$$

7. INTRINSIC STATIONARITY (OF ORDER ZERO)

Note 42. The class of (weakly) stationary random fields may not be sufficiently general enough to model a large number of important applications. E.g., in certain applications, it has been noticed that the “underline process” we wish to model presents increments whose variance

$$\text{Var}(Z(s+h) - Z(s)) = \text{Var}(Z(s+h)) + \text{Var}(Z(s)) - 2\text{Cov}(Z(s+h), Z(s))$$

increases indefinitely with $|h|$; this “process” cannot be modeled within the class of (weakly) stationary random fields whose increments have bounded variance $\text{Var}(Z(s+h) - Z(s)) = 2(c(0) - c(h)) < 2c(0)$. Intrinsic stationary is a weaker assumption extending the class of models we can use.

Definition 43. A random field $(Z(s) : s \in \mathcal{S})$ is called intrinsic random field (i.r.f.) (or intrinsic stationary r.f.) if, for all $h \in \mathcal{H}$,

- (1) $E(Z(s+h) - Z(s))^2 < \infty$
- (2) $E(Z(s+h) - Z(s)) = \mu(h)$ for some function $\mu : \mathcal{H} \rightarrow \mathbb{R}$ (lag dependent)
- (3) $\text{Var}(Z(s+h) - Z(s)) = 2\gamma(h)$ for some function $\gamma : \mathcal{H} \rightarrow \mathbb{R}$ (lag dependent)

Example 44. The random field with covariance function

$$c(s, t) = \frac{1}{2} \left(\|s\|^{2H} + \|t\|^{2H} - \|t-s\|^{2H} \right), \quad H \in (0, 1)$$

is not stationary r.f. because

$$c(s, s+h) = \frac{1}{2} \left(\|s\|^{2H} + \|s+h\|^{2H} - \|h\|^{2H} \right)$$

for $h \in \mathcal{H}$ but it intrinsic r.f. because

$$\frac{1}{2} \text{Var}(Z(s+h) - Z(s)) = \frac{1}{2} (\text{Var}(Z(s)) + \text{Var}(Z(s+h)) - 2\text{Cov}(Z(s), Z(s+h))) = \frac{1}{2} \|h\|^{2H}$$

Example 45. For an i.r.f. $(Z(s) : s \in \mathcal{S})$ with $\mu(h) = 0$, it can be shown that

$$(7.1) \quad \text{Cov}(Z(t) - Z(s), Z(v) - Z(u)) = \gamma(t-u) + \gamma(s-v) - \gamma(s-u) - \gamma(t-u)$$

by taking expectations from

$$2(a-b)(c-e) = (a-e)^2 + (a-b)^2 - (b-c)^2 - (a-c)^2$$

Note 46. The price to be paid for i.r.f. offering a larger class of models by setting the assumptions on the increments only, is involve an indeterminacy regarding the actual r.f. $Z(s)$; E.g. i.r.f. $(Z(s) : s \in \mathcal{S})$ and $(Z(s) + U : s \in \mathcal{S})$ where U a single variable leave (2) and (3) in Def 43 unchanged. When this causes problems, usual trick are: (a) “registration” (Example 47), i.e. consider an additional non-used specific site $s_0 \in \mathcal{S}$ (called origin) at which a value is known $Z(s_0) = z_0$ and try to work out (b) impose restrictions int eh increments.

Example 47. To specify the moments of an i.r.f. $Z(s)$. Consider an origin $s_0 \in \mathcal{S}$ with known $Z(s_0) = z_0$, and specify the “registered” r.f. $\tilde{Z}(s) = z_0 + (Z(s) - Z(s_0))$. Then $E(\tilde{Z}(s)) = z_0 + \mu(s - s_0)$ and $\text{Cov}(\tilde{Z}(s), \tilde{Z}(t))$ computed from (7.1).

Example 48. Only the covariance of allowed linear combinations can be represented w.r.t. $\gamma(\cdot)$. I.e.

$$\text{Cov} \left(\sum_{i=1}^n a_i Z(s_i), \sum_{j=1}^m b_j Z(s_j) \right) = \sum_{i=1}^n a_i \sum_{j=1}^m b_j \text{Cov}(Z(s_i), Z(s_j))$$

assuming Z is i.r.f. hence covariogram may not be defined, we consider origin $s_0 \in \mathcal{S}$ with $Z(s_0)$ and we restrict to the sum-to-zero linear combinations. Hence, by (7.1)

$$\begin{aligned}\text{Cov} \left(\sum_{i=1}^n a_i Z(s_i), \sum_{j=1}^n b_j Z(s_j) \right) &= \sum_{i=1}^n a_i \sum_{j=1}^n b_j \text{Cov}(Z(s_i) - Z(s_0), Z(s_j) - Z(s_0)) \\ &= \sum_{i=1}^n a_i \sum_{j=1}^n b_j (\gamma(s_i - s_0) + \gamma(s_j - s_0) - \gamma(s_j - s_i)) \\ &= - \sum_{i=1}^n \sum_{j=1}^n a_i b_j \gamma(s_j - s_i)\end{aligned}$$

8. INCREMENTAL MEAN FUNCTION

Definition 49. Incremental mean function (or drift) of the intrinsic random field $(Z(s) : s \in \mathcal{S})$ is defined as $\mu : \mathcal{H} \rightarrow \mathbb{R}$ with $\mu(h) = E(Z(s+h) - Z(s))$.

Example 50. Let $(Z(s) : s \in \mathcal{S})$ be an intrinsic random field, the incremental drift is linear

$$(8.1) \quad \mu(h) = h^\top \beta$$

for some $\beta \in \mathbb{R}^d$. Indeed, it is

$$\begin{aligned}\mu(h+h') &= E(Z(s+h+h') - Z(s)) = E(Z(s+h) - Z(s)) + E(Z(s+h+h') - Z(s+h)) \\ &= \mu(h) + \mu(h'), \quad \forall h, h'.\end{aligned}$$

Since, $\mu(\cdot)$ is continuous and $\mu(0) = 0$, than $\mu(h)$ is linear wrt h .

9. SEMIVARIOGRAM

Note 51. A very informative tool about the behavior of the intrinsic random field is the semivariogram function defined below.

Definition 52. The semivariogram of an intrinsic random field $(Z(s) : s \in \mathcal{S})$ is defined as $\gamma : \mathcal{H} \rightarrow \mathbb{R}$, with

$$\gamma(h) = \frac{1}{2} \text{Var}(Z(s+h) - Z(s))$$

Definition 53. Variogram of an intrinsic random field $(Z(s) : s \in \mathcal{S})$ is called the quantity $2\gamma(h)$.

Note 54. A stationary random field with covariogram $c(\cdot)$ and mean μ is intrinsic stationary as well with semivariogram

$$(9.1) \quad \gamma(h) = c(0) - c(h),$$

and constant incremental mean $\mu(h) = \mu$.

Example 55. For the Gaussian covariance function (Ex. 34) the semivariogram is

$$\gamma(h) = c(0) - c(h) = \sigma^2 (1 - \exp(-\beta \|h\|_2^2))$$

Proposition 56. *Properties of semivariogram.* Let $(Z(s) : s \in \mathcal{S})$ be an intrinsic random field, then

- (1) It is $\gamma(h) = \gamma(-h)$, $\gamma(h) \geq 0$, and $\gamma(0) = 0$
- (2) Semivariogram is conditionally negative definite (c.n.d.): if for all $n \in \mathbb{N}$, $(a_1, \dots, a_n) \subseteq \mathbb{R}^n$ s.t. $\sum_{i=1}^n a_i = 0$, and for all $(s_1, \dots, s_n) \subseteq S^n$, it is

$$\sum_{i=1}^n \sum_{j=1}^n a_i a_j \gamma(s_i - s_j) \leq 0$$

10. BEHAVIOR OF SEMIVARIOGRAM OF INTRINSIC RANDOM FIELDS

Note 57. The semivariogram $\gamma(h)$ is very informative when plotted against the lag h . Below we discuss some of the characteristics of it, using Figure 10.1

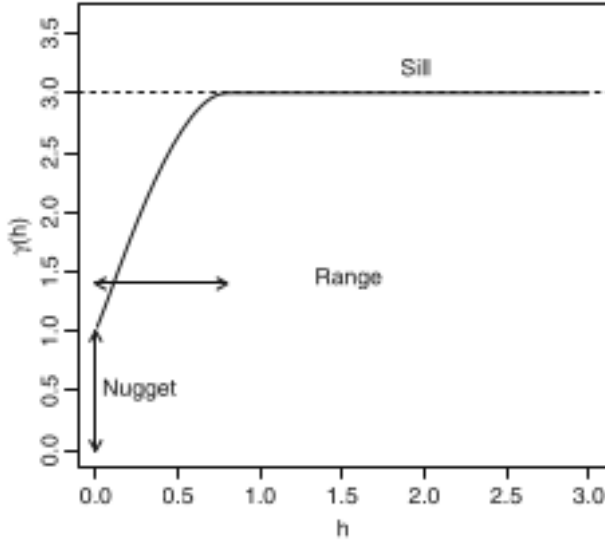


FIGURE 10.1. Semi Variogram's characteristics

Note 58. A semivariogram tends to be an increasing function of the lag $\|h\|$. Recall that for weakly stationary random fields with c.f. $c(\cdot)$, it is $\gamma(h) = c(0) - c(h)$ where common logic suggests that $c(h)$ is decreases with $\|h\|$.

Note 59. If $\gamma(h)$ is a positive constant for all non-zero lags $h \neq 0$, then $Z(s_1)$ and $Z(s_2)$ are uncorrelated regardless of how close s_1 and s_2 are. Then $Z(\cdot)$ is called white noise.

Note 60. Conversely, a non zero slope of the variogram indicates some structure.

Nugget Effect.

Note 61. Nugget effect is the semivariogram limiting value

$$\sigma_{\varepsilon}^2 = \lim_{\|h\| \rightarrow 0} \gamma(h)$$

when $\sigma_{\varepsilon}^2 \neq 0$.

Note 62. When used for modeling, nugget effect $\sigma_{\varepsilon}^2 \neq 0$ may express (1) measurement errors (e.g., if we collect repeated measurements at the same location s) or (2) some microscale variation causing discontinuity in the origin that cannot be detected from the data i.e. the spatial gaps because we collect a finite set of measurements at spatial locations. Ideally, a more detailed decomposition $\sigma_{\varepsilon}^2 = \sigma_{MS}^2 + \sigma_{ME}^2$ can be considered where σ_{MS}^2 refers to the microscale and σ_{ME}^2 refers to the measurement error. However this may lead to non-identifiability, without any obvious tweak to address it.

Sill.

Definition 63. Sill is the semivariogram limiting value $\lim_{\|h\| \rightarrow \infty} \gamma(h)$.

Note 64. For intrinsic processes, the sill may be infinite or finite. For weakly random field, the sill is always finite.

Partial sill .

Definition 65. Partial sill is $\lim_{\|h\| \rightarrow \infty} \gamma(h) - \lim_{\|h\| \rightarrow 0} \gamma(h)$ which takes into account the nugget.

Range .

Note 66. Range is the distance at which the semivariogram reaches the Sill. It can be infinite or finite.

Other.

Note 67. An abrupt change in slope indicates the passage to a different structuration of the values in space. This is often modeled via decomposition of processes with different semivariograms. E.g., let independent random fields $Y(\cdot)$ and $X(\cdot)$ with different semivariograms γ_Y and γ_X , then random field $Z(\cdot)$ with $Z(s) = Y(s) + X(s)$ has semivariogram $\gamma_Z(h) = \gamma_Y(h) + \gamma_X(h)$ which may present such a behavior.

11. ISOTROPY

Note 68. Isotropy introduces the assumption of “rotation invariance”.

Note 69. Isotropy applies to both intrinsic and (weakly) stationary random fields.

Definition 70. An intrinsic random field $(Z(s) : s \in \mathcal{S})$ is isotropic iff

$$(11.1) \quad \forall s, t \in \mathcal{S}, \frac{1}{2}\text{Var}(Z(s) - Z(t)) = \gamma(\|t - s\|), \text{ for some function } \gamma: \mathbb{R}_{\geq 0} \rightarrow \mathbb{R}.$$

Definition 71. Isotropic semivariogram $\gamma : \mathcal{H} \rightarrow \mathbb{R}$ is the semivariogram of the isotropic random field (sometimes for simplicity of notation we use $\gamma : \mathbb{R}_{\geq 0} \rightarrow \mathbb{R}$ with $\gamma(\|h\|) = \frac{1}{2}\text{Var}(Z(s) - Z(s - h))$).

Definition 72. Isotropic covariance function $C : \mathcal{S} \times \mathcal{S} \rightarrow \mathbb{R}$ is called the covariance function satisfying (11.1).

Definition 73. Isotropic covariogram $c : \mathcal{H} \rightarrow \mathbb{R}$ of a weakly stationary process is the covariogram associated to an isotropic semivariogram. Sometimes for simplicity of notation we use $c : \mathbb{R}_{\geq 0} \rightarrow \mathbb{R}$ with $c(\|h\|)$ from (11.1).

11.1. Popular isotropic covariance functions.

Note 74. Isotropic semivariograms can be computed from $\gamma(h) = c(0) - c(h)$ given covariogram $c(\cdot)$ for any h .

11.1.1. Nugget-effect.

Note 75. Nugget-effect covariogram takes the form

$$c(h) = \sigma^2 1_{\{0\}}(\|h\|)$$

for $\sigma^2 > 0$. It is associate to white noise. It is used to model a discontinuity in the origin of the covariogram / sem-variogram.

11.1.2. Matern c.f.

Note 76. Matern covariogram takes the form

$$(11.2) \quad c(h) = \sigma^2 \frac{2^{1-\nu}}{\Gamma(\nu)} \left(\frac{\|h\|}{\phi} \right)^\nu K_\nu \left(\frac{\|h\|}{\phi} \right)$$

for $\sigma^2 > 0$, $\phi > 0$, and $\nu \geq 0$. Parameter ν controls the variogram's regularity at 0 which in turn controls the quadratic mean (q.m.) regularity of the associated process. For $\nu = 1/2$, we get the exponential c.f.,

$$c(h) = \sigma^2 \exp \left(-\frac{1}{\phi} \|h\|_1 \right)$$

which is not differentiable at $h = 0$, while for $\nu \rightarrow \infty$, we get the Gaussian c.f.

$$c(h) = \sigma^2 \exp \left(-\frac{1}{\phi} \|h\|_2^2 \right)$$

which is infinite differentiable. ϕ is a range parameter, and σ^2 is the (partial) sill parameter.

No need to
memorize
(11.2)

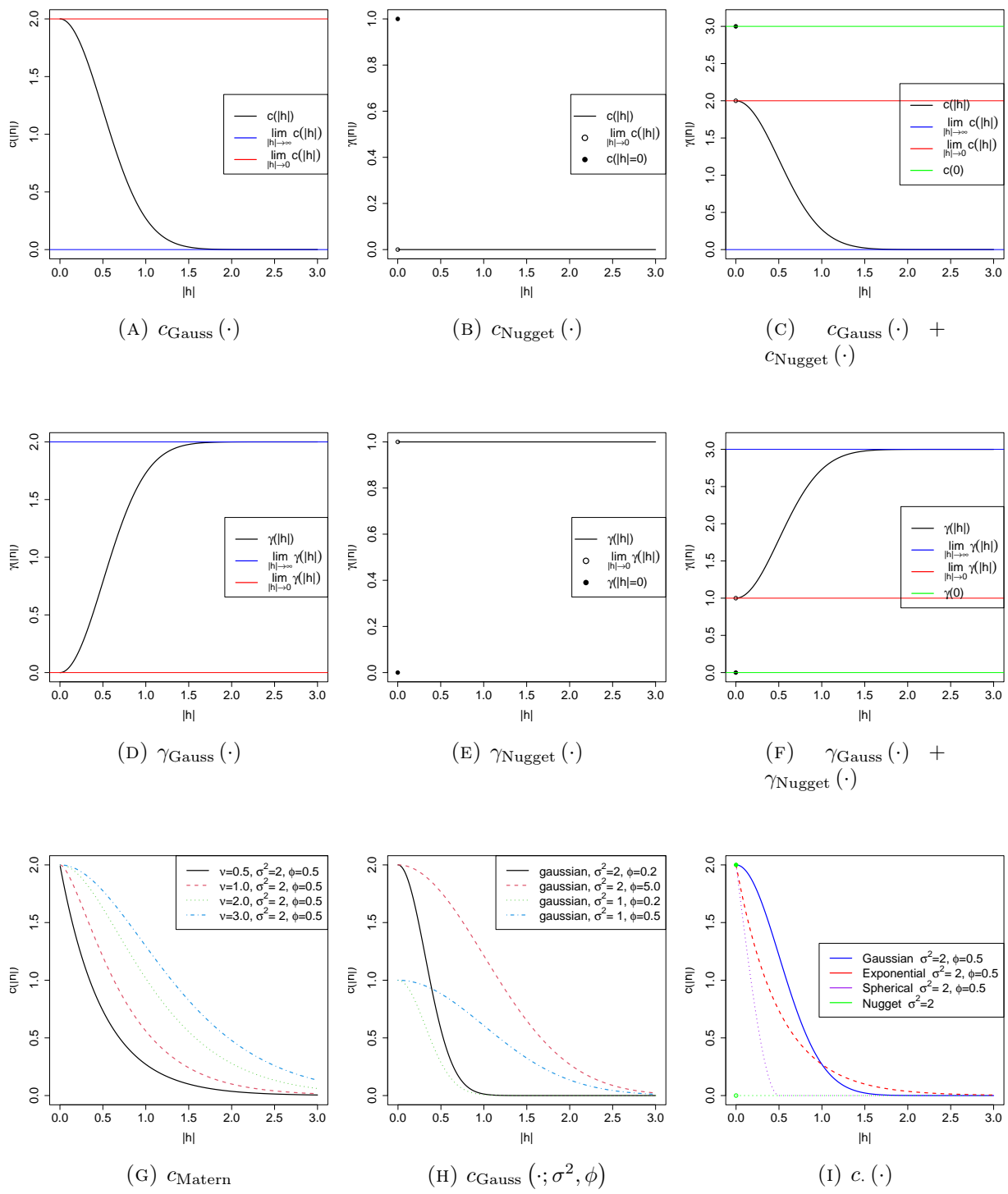


FIGURE 11.1. Covariogrames $c(\cdot)$ and semivariogrames $\gamma(\cdot)$

11.1.3. Spherical c.f.

Note 77. ¹Spherical covariogram takes the form

$$(11.3) \quad c(h) = \begin{cases} \sigma^2 \left(1 - \frac{3}{2} \frac{\|h\|_1}{\phi} + \frac{1}{2} \left(\frac{\|h\|_1}{\phi} \right)^3 \right) & \|h\|_1 \leq \phi \\ 0 & \|h\|_1 > \phi \end{cases}, \quad h \in \mathbb{R}^3.$$

for $\sigma^2 > 0$ and $\phi > 0$. The c.f. starts from its maximum value σ^2 at the origin, then steadily decreases, and finally vanishes when its range ϕ is reached. ϕ is a range parameter, and σ^2 is the (partial) sill parameter.

12. ANISOTROPY

Note 78. Dependence between $Z(s)$ and $Z(s+h)$ is a function of both the magnitude and the direction of separation h . This can be caused by the underlying physical process evolving differently in space (e.g., vertical and horizontal axes).

Definition 79. The semivariogram $\gamma : \mathcal{H} \rightarrow \mathbb{R}$ is anisotropic if there are h_1 and h_2 with same length $\|h_1\| = \|h_2\|$ but different direction $h_1/\|h_1\| \neq h_2/\|h_2\|$ that produce different semivariograms $\gamma(h_1) \neq \gamma(h_2)$.

Definition 80. The intrinsically random field $(Z(s) : s \in \mathcal{S})$ is anisotropic if its semivariogram is anisotropic.

Definition 81. The covariogram $c : \mathcal{H} \rightarrow \mathbb{R}$ is anisotropic if there are h_1 and h_2 with same length $\|h_1\| = \|h_2\|$ but different direction $h_1/\|h_1\| \neq h_2/\|h_2\|$ that produce different covariogram $c(h_1) \neq c(h_2)$.

Definition 82. The (weakly) stationary random field $(Z(s) : s \in \mathcal{S})$ is anisotropic if its covariogram is anisotropic.

Note 83. For brevity, below we discuss about intrinsic random fields and semivariograms, however the concepts/definitions apply to stationary random fields and covariograms when defined, as in Defs 79 & 81.

12.1. Geometric anisotropy.

Definition 84. The semivariogram $\gamma_{g.a.} : \mathcal{H} \rightarrow \mathbb{R}$ exhibits geometric anisotropy if it results from an A -linear deformation of an isotropic semivariogram with function $\gamma_{iso}(\cdot)$; i.e.

$$\gamma_{g.a.}(h) = \gamma_{iso}(\|Ah\|_2)$$

Note 85. Such semivariograms have the same sill in all directions but with ranges that vary depending on the direction. See Figure 12.1a.

¹For its derivation see Ch 8 in [4]

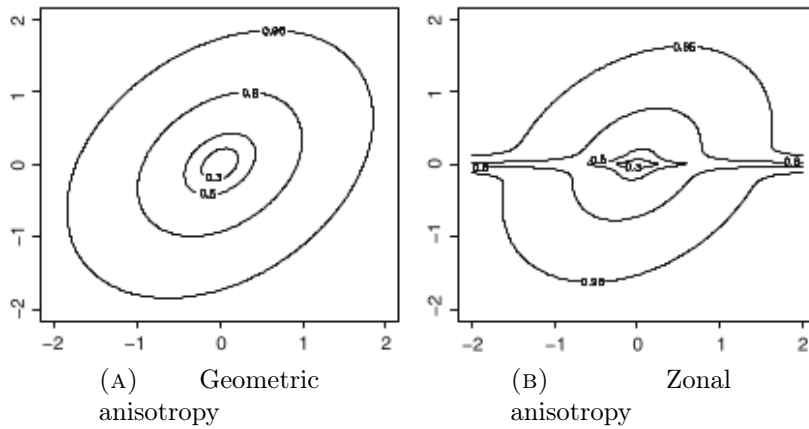


FIGURE 12.1. Isotropy vs Anisotropy

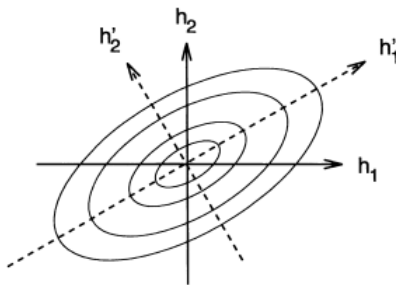


FIGURE 12.2. Rotation of the 2D coordinate system

Example 86. For instance, if $\gamma_{\text{g.a.}}(h) = \gamma_{\text{iso}}(\sqrt{h^\top Q h})$, where $Q = A^\top A$.

Example 87. [Rotating and dilating an ellipsoid in 2D] Consider a coordinate system for $h = (h_1, \dots, h_n)^\top$. We wish to find a new coordinate system for h in which the iso-semivariogram lines are spherical.

(1) [Rotate] Apply rotation matrix R to h such as $h' = Rh$. In 2D, it is

$$R = \begin{bmatrix} \cos(\theta) & \sin(\theta) \\ -\sin(\theta) & \cos(\theta) \end{bmatrix}, \text{ for } \theta \in (0, 2\pi), \text{ is the rotation angle.}$$

(2) [Dilate] Apply a dilation of the principal axes of the ellipsoid using a diagonal matrix $\sqrt{\Lambda} = \text{diag}(\sqrt{\lambda_1}, \dots, \sqrt{\lambda_n})$, as $\tilde{h} = \sqrt{\Lambda}h'$.

Now the ellipsoids become spheres with radius $r = \|\tilde{h}\|_2 = \sqrt{\tilde{h}^\top \tilde{h}}$. This yields the equation of an ellipsoid in the h coordinate system

$$h^\top (R^\top \Lambda R) h = r^2$$

where the diameters d_j (principal axes) of the ellipsoid along the principal directions are

$$d_j = 2r/\sqrt{\lambda_j}$$

and the principal direction is the j -th column of the rotation matrix $R_{\cdot,j}$.

Hence the anisotropic semivariogram is $\gamma_{\text{g.a.}}(h) = \gamma_{\text{iso}}(\sqrt{h^\top Q h})$ with $Q = R^\top \Lambda R$. This derivation extends to d dimensions.

12.2. Zonal (or stratified) anisotropy.

Definition 88. Support anisotropy is called the type of anisotropy that the semivariogram $\gamma(h)$ depends only on certain coordinates of h .

Example 89. If it is $\gamma(h = (h_1, h_2)) = \gamma(h_1)$, then I've support anisotropy

Definition 90. Zonal anisotropy occurs when the semivariogram $\gamma(h)$ is the sum of several components each with a support anisotropy.

Example 91. Let γ' and γ'' be semivariogram with sills v' and v'' correspondingly. If it is $\gamma(h = (h_1, h_2)) = \gamma'(\|h_1\|) + \gamma''(\sqrt{\|h_1\| + \|h_2\|})$, then I've Zonal anisotropy because γ has a sill $v' + v''$ in direction $(0, 1)$ and a sill v' in direction $(1, 0)$.

Note 92. We have Zonal anisotropy then the semivariogram calculated in different directions suggest a different value for the sill (and possibly the range).

Note 93. If in 2D case, the sill in h_1 is larger than that in h_2 , we can model zonal anisotropy of random field $(Z(s) : s \in \mathcal{S})$ by assuming $Z(s) = I(s) + A(s)$, where $I(s)$ is an isotropic random field with isotropic semivariogram γ_I along dimension of h_1 and $A(s)$ is an process with anisotropic semivariogram γ_A without effect on dimension h_1 ; i.e. $\gamma_Z(h) = \gamma_I(h) + \gamma_A(h)$.

12.3. Non-linear deformations.

Note 94. A (rather too general) non-stationary non-intrinsic random field model can be specified by considering semivariogram $2\text{Var}(Z(s) - Z(t)) = 2\gamma_o(\|G(s) - G(t)\|)$ such that a bijective non-linear (function) deformation $G(\cdot)$ of space \mathcal{S} has been applied on the isotropic semivariogram γ_o . For instance, $\gamma_o(h) = \sigma^2 \exp(-\|h\|/\phi)$ and $G(s) = s^2$ as a deterministic function. Now, if function $G(\cdot)$ is considered as unknown, one can model it as a random field $(G(s) : s \in \mathcal{S})$ with semivariogram $2\text{Var}(G(s) - G(t)) = 2\gamma'_o(\|G'(s) - G'(t)\|)$ and so on...; then we will be talking about deep learning.

13. GEOMETRICAL PROPERTIES OF RANDOM FIELDS

Note 95. We discuss basic geometric properties of random field we will use for modeling, as it can give us a deeper intuition on how to design appropriate spatial statistical models.

Definition 96. (Continuity in quadratic mean (q.m.)) Second-order random field $(Z(s) : s \in \mathcal{S})$ is q.m. continuous at $s \in \mathcal{S}$ if

$$\lim_{h \rightarrow 0} E(Z(s+h) - Z(s))^2 = 0.$$

Note 97. Consider random field $(Z(s) : s \in \mathcal{S})$. Then

$$E(Z(s+h) - Z(s))^2 = (E(Z(s+h)) - E(Z(s)))^2 + \text{Var}(Z(s+h) - Z(s))$$

- If Z is intrinsic r.f., then

$$E(Z(s+h) - Z(s))^2 = \frac{1}{2}\gamma(h)$$

and hence Z is q.m. continuous iff $\lim_{\|h\| \rightarrow 0} \gamma(h) = \gamma(0)$.

- If Z is stationary r.f., then

$$E(Z(s+h) - Z(s))^2 = \frac{1}{2}(c(0) - c(h))$$

and hence Z is q.m. continuous iff $\lim_{\|h\| \rightarrow 0} c(h) = c(0)$ (i.e. , c is continuous).

Definition 98. Differentiable in quadratic mean (q.m.)) Second-order random field $(Z(s) : s \in \mathcal{S})$ is q.m. differentiable at $s \in \mathcal{S}$ there exist

$$(13.1) \quad \dot{Z}(s) = \lim_{h \rightarrow 0} \frac{Z(s+h) - Z(s)}{h}. \text{ in q.m.}$$

Proposition 99. Let $c(s, t)$ be the covariance function of $Z = (Z(s) : s \in \mathcal{S})$. Then Z is everywhere differentiable if $\frac{\partial^2}{\partial s \partial t} c(s, t)$ exists and it is finite. Also, $\frac{\partial^2}{\partial s \partial t} c(s, t)$ is the covariance function of (13.1).

Example 100. The process with exponential c.f. $c(h) = \sigma^2 \exp(-|h|/\phi)$ is continuous because $\lim_{h \rightarrow 0} c(h) = \sigma^2 = c(0)$ but not differentiable because $\frac{\partial^2}{\partial h^2} c(h)$ does not exist at $h = 0$.

Part 2. Model building & related parametric inference

14. THE GEOSTATISTICAL MODEL (THE BIG PICTURE)

14.1. Linear Model of Regionalization.

Note 101. A spatial phenomenon can be thought as being the sum of several independent subphenomena acting at different characteristic scales. A linear model can be set up to split the stochastic process representing the phenomenon into several uncorrelated stochastic processes, each with a different variogram or covariance function and characterizing different aspect of the overall phenomenon under investigation.



FIGURE 14.1. Variogram $\gamma(\cdot)$ of $Z(s) = Z_1(s) + Z_2(s) + Z_3(s)$ with spherical s.v. $\gamma_1(|h|; \sigma^2 = 0.8, \phi = 3.5)$, spherical s.v. $\gamma_1(|h|; \sigma^2 = 1.1, \phi = 6.5)$, and nugget $\gamma_3(|h|; \sigma^2 = 0.4)$.

14.1.1. Decomposition of the random field.

Note 102. The linear model of regionalization consider the decomposition of the random field of interest $Z(s)$ as a summation of m independent zero-mean random fields $\{Z_j(s); s \in \mathcal{S}\}_{j=0}^m$ each of them characterizing different spatial scales, as

$$(14.1) \quad Z(s) = \mu(s) + Z_1(s) + \dots + Z_m(s)$$

with $\mu(s) = E(Z(s))$ be a deterministic drift (or trend) function.

Remark 103. In (14.1), let $Z_j(\cdot)$ be intrinsic random field with semivariogram $\gamma_j(\cdot)$ and mutually independent, then the semivariogram of $Z(\cdot)$ is $\gamma(\cdot) = \sum_{j=1}^m \gamma_j(\cdot)$.

Example 104. For instance consider (14.1) with $\mu(s) = 0$, $m = 3$, $Z_1(s)$ with a spherical semivariogram (11.3) with range $\phi_1 = 3.5$, $Z_2(s)$ with a spherical semi-variogram (11.3) with range $\phi_2 = 6.5$, and $Z_3(s)$ with a nugget semi-variogram. See the “sudden” changes of the line in Figure 14.1 representing change of spatial behavior.

14.1.2. Scale of variation.

Note 105. Cressi [1] considers the following intuitive decomposition

$$(14.2) \quad Z(s) = \mu(s) + W(s) + \eta(s) + \varepsilon(s), \quad s \in S$$

where

Page 21

Created on 2024/10/30 at 13:33:05

by Georgios Karagiannis

$\mu(s) = \mathbf{E}(Z(s))$: is the deterministic mean (or drift) structure. It aims to represent the “large scale variation”.

$W(s)$: is a zero mean second order continuous intrinsic random field whose range is larger than gaps between the sites (sampling grid). It aims to represent “smooth small scale variation”.

$\eta(s)$: is a zero mean intrinsic random field whose variogram range exists and is smaller than the gaps between the sites. It aims to represent “microscale variation”

$\varepsilon(s)$: is a zero-mean white-noise process (modeled as nugget effect). It aims to represent “measurement error or noise”

$W(s), \eta(s), \varepsilon(s)$ are mutually independent.

Note 106. Reasonably, larger scale components, such as $\mu(s), W(s)$ can be represented in the variogram if the diameter of the sampling domain is large S is large enough.

Note 107. Clearly, smaller scale components, such as $\eta(s), \varepsilon(s)$ could be identified if the sampling grid is sufficiently fine.

Note 108. Decomposition (14.2) is not unique and the components are not clearly identifiable from the data when modeled; e.g. one may find two pairs of $\mu(s), W(s)$ doing the same thing; yet, separating $\eta(s)$ and $\varepsilon(s)$ is difficult as they often describe changes with range smaller than that of the sites (!)

Note 109. The geostatistical model is often presented (with reference to (14.2)) is a form

$$Z(s) = \mu(s) + w(s) + \varepsilon(s), \quad s \in S$$

where $w(s) = W(s) + \eta(s)$ contains all the spatial variation.

Note 110. Alternatively, the hierarchical statistical model (Handout 1, 3.5) is used

$$(14.3) \quad Z(s) = Y(s) + \varepsilon(s), \quad s \in S$$

where $Y(s) = \mu(s) + W(s) + \eta(s)$ is the spatial model, signal random field or noiseless random field.

Note 111. Another decomposition we will use

$$Z(s) = \mu(s) + \delta(s), \quad s \in S$$

where $\delta(s) = W(s) + \eta(s) + \varepsilon(s)$ is the called the correlated process.

Note 112. In several problems, additional covariates may be considered. The available dataset is of the form $\{(x_i, s_i, Z_i)\}_{i \in S}$ where $Z_i := Z(s_i, x_i)$ is the observed response at

location s_i , associated with the p -dimensional covariate $x_i = (x_{i,1}, \dots, x_{i,p})^\top$ for $i \in \mathcal{S}$. Although not a necessity rule, the effect of the associated p -dimensional covariates is often expressed via the deterministic drift function $\mu(s, x) = E(Z(s, x))$. E.g. in decomposition in (14.2)

$$(14.4) \quad Z(s, x) = \mu(s, x) + W(s) + \eta(s) + \varepsilon(s), \quad s \in S, x \in \mathcal{X}.$$

Here, to simplify the presentation, we suppress dependence on possible covariates $x \in \mathcal{X}$.

15. LEARNING THE SEMIVARIOGRAM

Note 113. Consider a random field $(Z(s); s \in \mathcal{S})$, $\mathcal{S} \in \mathbb{R}^d$ observed at n sites $S = \{s_1, \dots, s_n\}$, and hence a dataset $\{(s_i, Z(s_i))\}_{i=1}^n$.

Note 114. Consider a decomposition

$$Z(s) = \mu(s) + \delta(s), \quad s \in S$$

where $\mu(\cdot)$ is an unknown deterministic drift and $\delta(\cdot)$ is a zero mean intrinsic random field.

Example 115. (Meuse river data set) The Meuse river dataset set, used as a running example gives locations and topsoil heavy metal concentrations, along with a number of soil and landscape variables at the observation locations, collected in a flood plain of the river Meuse, near the village of Stein (NL). Here, we use the topsoil zinc concentration, mg kg⁻¹ soil ("ppm") as quantity of interest (Z). See Figure 15.1a. This is the R dataset `meuse{sp}`.

Example 116. (Wolfcamp-aquifer dataset) We also consider the Wolfcamp-aquifer dataset in Exercise 2 in the Exercise sheet. See Figure 15.2a

15.1. The semvariogram cloud.

Assumption 117. Assume that $(Z(s); s \in \mathcal{S})$ in an intrinsic random field with unknown constant mean; aka $Z(s) = \mu + \delta(s)$.

Definition 118. Dissimilarity between pairs of data values $Z(s_a)$ and $Z(s_b)$ is called the measure

$$(15.1) \quad \gamma^*(s_a, s_b) = \frac{1}{2} (Z(s_b) - Z(s_a))^2$$

Definition 119. If we let dissimilarity between pairs of data values $Z(s)$ and $Z(s_b)$ depend on the separation $h = s_b - s$ (lag or orientation) then we get

$$\gamma^*(h) = \frac{1}{2} (Z(s+h) - Z(s))^2.$$

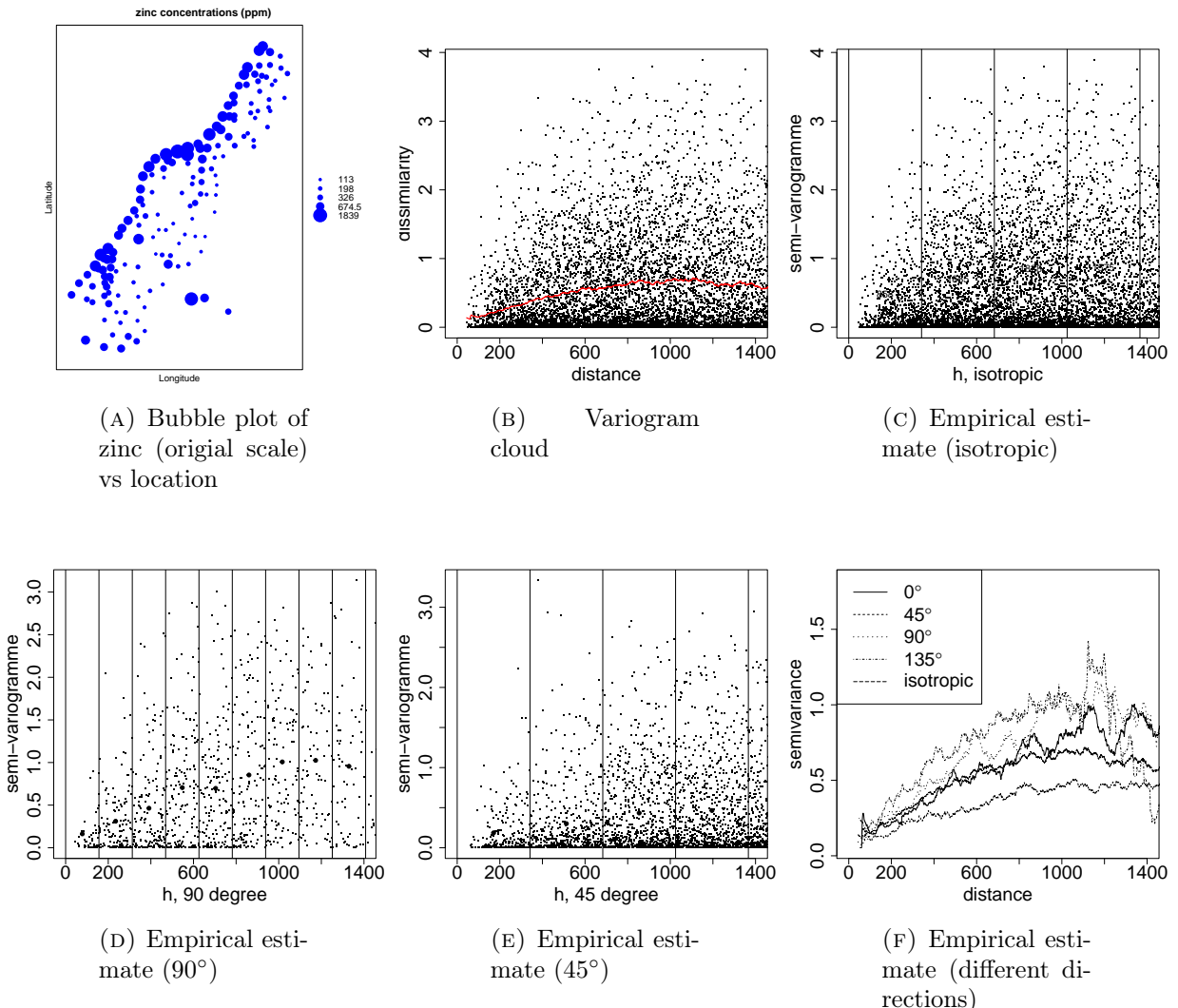


FIGURE 15.1. Meuse dataset variogram estimations (Zinc in log scale)

Definition 120. The semivariogram cloud is the set of $n(n - 1)/2$ points

$$\mathfrak{C}_S = \{(\|s_i - s_j\|, \gamma^*(s_j, s_i)), i, j = 1, \dots, n, \text{ and } s_i \neq s_j\}$$

Note 121. Note that (15.1) is an unbiased estimator of the semivariogram and hence the semivariogram cloud is too.

Note 122. Often there is a smoothing of the cloud is superimposed onto the cloud itself to help us see semivariogram's characteristics (e.g., sill, nugget, range) which may be “hidden” due to potential outliers in the plot.



FIGURE 15.2. Wolfcamp-aquifer dataset variogram estimations

Example 123. Figure 15.1b and Figure 15.2b show the semivariogram cloud plots (that is a point plot of the dissimilarities vs the distances) for the datasets Meuse and Wolfcamp-aquifer dataset. The red line is a smoother line of the cloud.

15.2. Non-parametric semivariogram estimator of $\gamma(\cdot)$.

Assumption 124. Assume that $(Z(s); s \in \mathcal{S})$ in an intrinsic random field with unknown constant mean; aka $\mu(\cdot)$ is an unknown constant.

Proposition 125. The Smoothed Matheron estimator $\hat{\gamma}(\cdot)$ of semivariogram $\gamma(\cdot)$ of an unknown constant mean intrinsic random field $Z(\cdot)$ is

$$(15.2) \quad \hat{\gamma}_M(h) = \frac{1}{2|N_{r_1, r_2}(h)|} \sum_{\forall(s_i, s_j) \in N_{r_1, r_2}(h)} (Z(s_i) - Z(s_j))^2$$

where

$$N_{r_1, r_2}(h) = \{(s_i, s_j) \in \mathcal{S} : s_i - s_j \in B_{r_1, r_2}(h)\}$$

contains all the pairs of spatial points points whose difference is in a ball

$$(15.3) \quad B_{r_1, r_2}(h) = \left\{ x : \| \|x\| - \|h\| \| < r_1, \text{ and } \left\| \frac{x}{\|x\|_2} - \frac{h}{\|h\|_2} \right\|_2 < r_2 \right\}$$

centered at h with radius $r_1 > 0$ and $r_2 > 0$.

Note 126. If we consider isotropic semivariogram $\gamma(\cdot)$ then the ball may just considerate only the length of the distance as

$$(15.4) \quad B_{r_1}(h) = \{x : \| \|x\| - \|h\| \| < r_1\}$$

because the direction does not have any effect.

Note 127. The choice of r_1, r_2 is an art, and a trade-off between variance and bias, similar to the bin length in histograms.

Note 128. In practice, we consider a finite number of k separations $\mathcal{H} = \{h_1, \dots, h_k\}$, we estimate in such a way that each class contains at least 30 pairs of points. Then compute $\{\hat{\gamma}_M(h) ; h \in \mathcal{H}\}$, and plot $\{(h_j, \hat{\gamma}_M(h_j)) ; j = 1, \dots, k\}$.

Example 129. Figures 15.1c and 15.2c, show the nonparametric estimator ignoring the direction for the datasets Meuse and Wolfcamp-aquifer dataset. The estimator is calculated by using the ball in (15.4).

Example 130. Figures 15.2d and 15.1e show the nonparametric estimator considering directions 90° and 45° for the dataset Meuse. Figures 15.2d and 15.2e do the same for the Wolfcamp-aquifer dataset. The estimator is calculated by using the ball (15.3).

Note 131. In practice anisotropies are detected by inspecting experimental semivariograms in different directions and are induced into the model by tuning predefined anisotropy parameters.

Example 132. Figure 15.1f and 15.2a show the nonparametric semivariogram estimator for different directions for the two datasets. We observe possible anisotropy due to the differences in the lines.

15.3. Classic parametric estimator of $\gamma(\cdot)$.

Assumption 133. Consider (for now) the assumption that $(Z(s) ; s \in \mathcal{S})$ in an intrinsic random field with unknown constant mean; aka $\mu(\cdot)$ is an unknown constant.

Note 134. Smoothed Matheron estimator (15.2) does not necessarily satisfies semivariogram properties, such as negative definiteness. To address this we use a parametric family of appropriate semi-variogram functions and tune them against data.

Note 135. Popular parametrized isotropic semivariograms are those Section 11.1. Anisotropic semi-variograms/covariograms can be specified by using isotropic ones and applying a rotation and dilation as in Example 86.

Note 136. Below are some properties that allow the specification of sophisticated semivariograms from simpler ones.

- (1) $\tilde{\gamma}(h) = \gamma(Ah)$ where $\gamma(\cdot)$ is a semivariogram and A constant matrix.
- (2) $\gamma(\cdot) = \sum_{i=1}^n a_i \gamma_i(\cdot)$, if $a_i \geq 0$, and $\{\gamma_i(\cdot)\}$ are semivariograms
- (3) $\gamma(\cdot) = \prod_{i=1}^n \gamma_i(\cdot)$, if $\{\gamma_i(\cdot)\}$ are semivariograms
- (4) $\gamma(\cdot) = \int \gamma_u(\cdot) dF(u)$, if $\gamma_u(\cdot)$ is a semivariogram parametrized by $u \sim F$
- (5) $\gamma(\cdot) = \lim_{n \rightarrow \infty} \gamma_n(\cdot)$ if $\gamma_n(\cdot)$ is semivariogram and the limit exists
- (6) $\gamma_Z(h) = \gamma_Y(h) + \gamma_X(h)$ corresponds to random field $Z(s) = Y(s) + X(s)$ if $(Y(s) : s \in \mathcal{S})$ and $(X(s) : s \in \mathcal{S})$ are independent intrinsic random fields with semi-variograms $\gamma_Y(\cdot)$ and $\gamma_X(\cdot)$.
- (7) $\gamma(\cdot)$ is a semivariogram iff $\exp(-a\gamma(\cdot))$ is positive definite for any $a > 0$.

Example 137. $\gamma(h) = \|h\|^2$ is a semivariogram because $\exp(-a\|h\|_2^2)$ is a c.f. for any $a > 0$ and hence positive definite.

Note 138. For a q.m. continuous $(Z(s) : s \in \mathcal{S})$, it is $\lim_{\|h\| \rightarrow 0} \gamma(h) = 0$ because $\gamma(0) = 0$. However, when modeling a real problem we may need to consider (or it may appear from the data) that $\gamma(h)$ should have a discontinuity $\lim_{\|h\| \rightarrow 0} \gamma(h) = \sigma_\varepsilon^2 \neq 0$ aka a nugget. Nugget [5; effect is often mathematically described by considering a decomposition ; Ch 1.4.1]

$$Z(s) = Y(s) + \varepsilon(s)$$

where Y can be a continuous random field with $\gamma_Y(\cdot)$, and ε can be a random field (called errors-in-variables model) with (nugget) semivariogram $\gamma_\varepsilon(h) = \sigma_\varepsilon^2 \mathbf{1}(h \neq 0)$. In this case,

$$\gamma_Z(h) = \gamma_Y(h) + \gamma_\varepsilon(h) \xrightarrow{\|h\| \rightarrow 0} \sigma_\varepsilon^2$$

Note 139. Let $\hat{\gamma}$ be the empirical semivariogram $\hat{\gamma}$ (e.g., Matheron (15.2)) computed at k classes, i.e. it is available $\{h_j, \hat{\gamma}(h_j)\}_{j=1}^k$. Let γ_θ be a parametrised semivariogram by the unknown θ . The Least Square Errors (LSE) estimator is $\hat{\gamma}_{\text{LSE}}(h) = \gamma(h; \hat{\theta}_{\text{LSE}})$ where

$$(15.5) \quad \hat{\theta}_{\text{LSE}} = \arg \min_{\theta} (\hat{\gamma} - \gamma(h; \theta))^\top V(\theta) (\hat{\gamma} - \gamma(h; \theta)),$$

$V(\theta)$ is a user specific positive definite matrix $V(\theta)$ serving as a weight, $\hat{\gamma} = (\hat{\gamma}(h_1), \dots, \hat{\gamma}(h_k))^T$, and $\gamma(h; \theta) = (\gamma(h_1; \theta), \dots, \gamma(h_k; \theta))^T$.

Note 140. An example is OLS

$$(15.6) \quad \hat{\theta}_{\text{OLS}} = \arg \min_{\theta} \left(\sum_j (\hat{\gamma}(h_j) - \gamma(h; \theta))^2 \right)$$

Example 141. Figures 15.3a and 15.3b show the OLE and WLE estimates (15.6) and (7.5) of the exponential and spherical semivariogram for the Meuse dataset. Figure 15.3c shows the OLE and WLE estimates (15.6) and (7.5) of the exponential semi-variogram for the Wolfcamp dataset. The parametric semivariograms were tuned against the non-parametric estimator (15.2) presented in dots, as discussed in Proposition 139.

15.4. Parametric learning of nonzero $\mu(\cdot)$ and $\gamma(\cdot)$.

Note 142. Assume a random field model $(Z(s); s \in \mathcal{S})$ decomposed as

$$Z(s) = \mu(s) + \delta(s)$$

where the trend $\mu(s)$ is parameterized as $\mu(s) = \mu(s; \beta)$ with unknown β (e.g. $\mu(s; \beta) = \psi^\top(s) \beta$), and the zero mean intrinsic process $\delta(s)$ has a semivariogram $\gamma(h)$ parameterised as $\gamma(h) = \gamma(h; \theta)$ with unknown θ .

15.4.1. Non-parametric inference.

Note 143. Semi-parametric learning is as follows:

- (1) Compute estimate $\hat{\beta}$ via LSE (or equivalent)

$$(15.7) \quad \hat{\beta}_{\text{LSE}} = \arg \min_{\theta} \left(\sum_i (Z(s_i) - \mu(s_i; \beta))^2 \right)$$

- (2) Compute the residuals $\hat{\delta} := \hat{\delta}(s_i)$ from

$$(15.8) \quad \hat{\delta}(s_i) = Z(s_i) - \mu(s_i; \hat{\beta}_{\text{LSE}})$$

- (3) Compute empirical variogram against $\hat{\delta}$ on \mathcal{H} according to Proposition 125.
- (4) Compute estimates $\hat{\theta}_{\text{LSE}}$ and $\hat{\gamma}_{\text{LSE}}(h)$ according to Proposition 139.

Example 144. Figure 15.3a and 15.3b fit an exponential c.f. and a spherical c.f. in the data of Meuse dataset (assuming constant mean); we cannot eyeball any big difference. Figure 15.3c fit an exponential c.f. in the data of Wolfcamp dataset (assuming constant mean); the fit looks really bad, possibly we should consider a non-constant mean and remove the trend.



FIGURE 15.3. Parametric training

Example 145. Figure 15.3d fits an exponential c.f. in the residuals $\delta(s) = Z(s) - \mu(s)$ where $\mu(s) = \beta_0 + \beta_1 s_1 + \beta_2 s_2$ and $\hat{\beta}_{OLS} = (-42.8, -9.5 \cdot 10^{-4}, -6.6 \cdot 10^{-4})^\top$ in Meuse dataset. Possibly inference would suggest a constant mean function. Figure 15.3e fits an exponential c.f. in the residuals $\delta(s) = Z(s) - \mu(s)$ where $\mu(s) = \mu(s) = \beta_0 + \beta_1 s_1 + \beta_2 s_2$ and $\hat{\beta}_{OLS} = (-607, -1.12, -1.13)^\top$ in Wolfcamp dataset; we see an improvement in fit compared to Figure 15.3c.

15.4.2. Parametric inference via MLE.

Note 146. Assume that the probability distribution of the random field $(Z(s); s \in \mathcal{S})$ is known. The MLE estimates $(\hat{\beta}_{MLE}, \hat{\theta}_{MLE})$ of (β, θ) can be computed as

$$(\hat{\beta}_{MLE}, \hat{\theta}_{MLE}) = \arg \min_{(\beta, \theta)} (-2 \log (L(z_1, \dots, z_n | \beta, \theta)))$$

where $L(z_1, \dots, z_n | \beta, \theta)$ is the associated likelihood function given observed data $\{(s_i, Z_i)\}_{i=1}^n$.

Example 147. If $Z(\cdot) \sim GP(\mu(\cdot; \beta), c(\cdot, \cdot; \sigma^2, \phi))$, with $\mu(s; \beta) = \beta_0 + s_1\beta_1 + s_2\beta_2$ and $c_{(\sigma^2, \phi)}(h) = \sigma^2 (1 - \exp(-\phi h^2))$ then MLE of (β, σ^2, ϕ) is

$$(\hat{\beta}_{MLE}, \hat{\sigma}_{MLE}^2, \hat{\phi}_{MLE}) = \arg \min_{\beta, \sigma^2, \phi} (-2 \log (N(Z | \mu_\beta, C_{\sigma^2, \phi})))$$

where $N(Z | \mu_\beta, C_\theta)$ is the Gaussian pdf at $Z = (Z(s_1), \dots, Z(s_n))^\top$, with mean $[\mu_\beta]_i = \mu(s_i; \beta) = \beta_0 + s_{1,i}\beta_1 + s_{2,i}\beta_2$ and covariance matrix $[C_{\sigma^2, \phi}]_{i,j} = \sigma^2 \exp(-\phi(s_i - s_j)^2)$.

16. (CLASSICAL) KRIGING (FOR PREDICTION)

Note 148. “Kriging” is a general technique for deriving an estimator / predictor of $Z(\cdot)$ (or a function of it) at a location (such as a spatial point s_0 , or a block of points $\{s_j^*\}$ or a subregion v_0) of a spatial region \mathcal{S} by properly averaging out data in the neighborhood around the location of interest.

16.1. Universal Kriging.

Note 149. Consider the statistical model specified as a stochastic process $(Z(s); s \in \mathcal{S})$ with

$$(16.1) \quad Z(s) = \mu(s) + \delta(s)$$

where $\mu(s)$ is a deterministic linear expansion of known basis functions $\{\psi_j(\cdot)\}_{j=0}^p$ and unknown coefficients $\{\beta_j\}_{j=0}^p$ such as

$$\mu(s) = \sum_{j=0}^p \psi_j(s) \beta_j = (\psi(s))^\top \beta$$

with $\beta = (\beta_0, \dots, \beta_p)^\top$ and $\psi(s) = (\psi_0(s), \dots, \psi_p(s))^\top$. Also, $\delta(s)$ is a zero mean random field.

Note 150. Consider an available a dataset $\{(s_i, Z_i)\}_{i=1}^n$ with $Z_i := Z(s_i)$ being a realization of $(Z(s); s \in \mathcal{S})$ at site s_i . At these dataset points (16.1) is vectorized as

$$Z = \mu + \delta = \Psi \beta + \delta$$

with vectors $Z = (Z(s_1), \dots, Z(s_n))^\top$, $\delta = (\delta(s_1), \dots, \delta(s_n))^\top$, and $\mu = (\mu(s_1), \dots, \mu(s_n))^\top$, and with (design) matrix Ψ such as $[\Psi]_{i,j} = \psi_j(s_i)$.

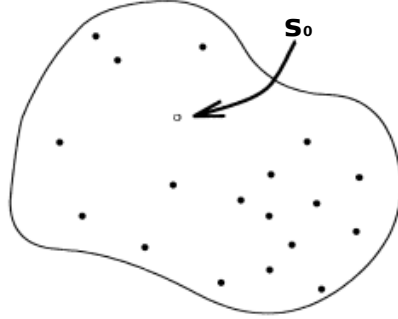


FIGURE 16.1. Kriging area

Note 151. Interested lies in learning/predicting $Z(s_0)$ at an unseen spatial location s_0 within the spatial domain \mathcal{S} (Figure 16.1).

Note 152. “Universal Kriging” (UK) is the technique for producing a Best Linear Unbiased Estimator (BLUE) predictor for $Z_0 := Z(s_0)$ at spatial location $s_0 \in \mathcal{S}$ as a weighted average of the available data around in a neighborhood around that location .

Definition 153. The Universal Kriging (UK) predictor $Z_{\text{UK}}(s_0)$ of $Z(s_0)$ at location $s_0 \in \mathcal{S}$ is the Best Linear Unbiased Estimator (BLUE) of $Z(s_0)$ given the data $\{(s_i, Z_i)\}_{i=1}^n$.

Note 154. [LINEAR] The UK predictor $Z_{\text{UK}}(s_0)$ of $Z(s_0)$ at s_0 has the following linear form weighted by a set of tunable unknown weights $\{w_i\}$

$$(16.2) \quad Z_{\text{UK}}(s_0) = w_{n+1} + \sum_{i=1}^n w_i Z(s_i)$$

$$(16.3) \quad = w_{n+1} + w^\top Z$$

where $Z = (Z_1, \dots, Z_n)^\top$ and $w = (w_1, \dots, w_n)^\top$.

Note 155. [Unbiased] For (16.2), to satisfy unbiasedness (that is zero systematic error”), we need

$$\begin{aligned} E(Z_{\text{UK}}(s_0)) &= E(Z(s_0)) \Leftrightarrow w_{n+1} + \sum_{i=1}^n w_i E(Z(s_i)) = \mu(s_0) \\ &\Leftrightarrow w_{n+1} + \sum_{i=1}^n w_i \mu(s_i) = \mu(s_0) \Leftrightarrow w_{n+1} + \sum_{i=1}^n w_i (\psi(s_i))^\top \beta = (\psi(s_0))^\top \beta \\ (16.4) \quad &\Leftrightarrow w_{n+1} + w^\top \Psi \beta = \Psi_0 \beta \end{aligned}$$

where Ψ is matrix with $[\Psi]_{i,j} = \psi_j(s_i)$ and Ψ_0 is a (column) vector with $[\Psi_0]_{1,j} = \psi_j(s_0)$. Because in (16.4) both sides are polynomial w.r.t β all coefficients must be equal; hence

sufficient and necessary conditions for unbiasedness are

$$(16.5) \quad \text{Assumption:} \quad (\psi(s_0))^\top = \sum_{i=1}^n w_i (\psi(s_i))^\top \Leftrightarrow \Psi_0 = w^\top \Psi$$

$$(16.6) \quad \text{Assumption:} \quad w_{n+1} = 0$$

Note 156. We set $\psi_0(\cdot) = 1$; then (16.4) implies

$$(16.7) \quad \text{Assumption:} \quad \sum_{i=1}^n w_i = 1 \Leftrightarrow w^\top \underline{1} = 1$$

Note 157. The MSE of $Z_{\text{UK}}(s_0)$, given some of the above Assumptions, is

$$(16.8) \quad \text{MSE}(Z_{\text{UK}}(s_0)) = E(Z_{\text{UK}}(s_0) - Z(s_0))^2 \\ = E(\Psi\beta + \delta(s_0) - w^\top \Psi\beta - w^\top \delta)^2; \quad \left\{ \text{let } \delta = (\delta(s_1), \dots, \delta(s_n))^\top \right\}$$

$$(16.9) \quad = E\left(\sum_{i=1}^n w_i \delta(s_i) - \delta(s_0)\right)^2 \stackrel{\sum_{i=1}^n w_i = 1}{=} E\left(\sum_{i=1}^n w_i (\delta(s_i) - \delta(s_0))\right)^2$$

$$(16.10) \quad = -E\left(\frac{1}{2} \sum_{i=1}^n \sum_{j=1}^n w_i w_j (\delta(s_i) - \delta(s_j))^2 - 2 \frac{1}{2} \sum_{i=1}^n w_i (\delta(s_i) - \delta(s_0))^2\right)$$

$$(16.11) \quad = -\sum_{i=1}^n w_i \sum_{j=1}^n w_j \frac{1}{2} E(\delta(s_i) - \delta(s_j))^2 + 2 \sum_{i=1}^n w_i \frac{1}{2} E(\delta(s_i) - \delta(s_0))^2$$

Note 158. To impose tractability, we consider the following additional assumption

$$(16.12) \quad \text{Assumption:} \quad (\delta(s); s \in \mathcal{S}) \text{ intrinsic random field with semivariogram } \gamma(\cdot)$$

Note 159. Since $(\delta(s); s \in \mathcal{S})$ is intrinsic stationary, and its semivariogram exists, $\text{MSE}(Z_{\text{UK}}(s_0))$ can be expressed w.r.t. the semivariogram as

$$(16.13) \quad \text{MSE}(Z_{\text{UK}}(s_0)) = -\sum_{i=1}^n w_i \sum_{j=1}^n w_j \gamma(s_i - s_j) + 2 \sum_{i=1}^n w_i \gamma(s_i - s_0)$$

$$(16.14) \quad = -w^\top \Gamma w + 2w^\top \gamma_0$$

where $w = (w_1, \dots, w_n)^\top$, $\gamma_0 = (\gamma(s_0 - s_1), \dots, \gamma(s_0 - s_n))^\top$, and $[\Gamma]_{i,j} = \gamma(s_i - s_j)$.

Note 160. [Best] The Lagrange function for minimizing the MSE (16.13) under (16.4) is

$$\begin{aligned} \mathfrak{L}(w, \lambda) &= -\sum_{i=1}^n \sum_{j=1}^n w_i w_j \gamma(s_i - s_j) + 2 \sum_{i=1}^n w_i \gamma(s_0 - s_i) - \sum_{j=0}^p \lambda_j \left(\sum_{i=1}^n w_i \psi_j(s_i) - \psi_j(s_0) \right) \\ &= -w^\top \Gamma w + 2w^\top \gamma_0 - (w^\top \Psi - \Psi_0) \lambda \end{aligned}$$

Note 161. The UK system of equations is

$$(16.15) \quad \begin{cases} 0 = \nabla_{(w,\lambda)} \mathfrak{L}(w, \lambda) \Big|_{(w_{\text{UK}}, \lambda_{\text{UK}})} \iff \\ \begin{aligned} 0 &= -2 \sum_{j=1}^n w_{\text{UK},j} \gamma(s_i - s_j) + 2\gamma(s_0 - s_i) - \sum_{j=0}^p \lambda_{\text{UK},j} \psi_j(s_i), \\ \psi_j(s_0) &= \sum_{i=1}^n w_{\text{UK},i} \psi_j(s_i), \quad j = 0, \dots, p \end{aligned} \end{cases} \quad i = 1, \dots, n \iff$$

$$(16.16) \quad \begin{cases} 0 = -2\Gamma w + 2\gamma_0 - \Psi \lambda_{\text{UK}} \\ \Psi_0 = w_{\text{UK}}^\top \Psi \end{cases}$$

Then by multiplying both sides by $\Psi^\top \Gamma^{-1}$ I get

$$(16.17) \quad \begin{aligned} 0 &= -2\Psi^\top \Gamma^{-1} \Gamma w_{\text{UK}} + 2\Psi^\top \Gamma^{-1} \gamma_0 - \Psi^\top \Gamma^{-1} \Psi \lambda_{\text{UK}} \iff \\ \lambda_{\text{UK}} &= 2(\Psi^\top \Gamma^{-1} \Psi)^{-1} (\Psi^\top \Gamma^{-1} \gamma_0 - \Psi_0^\top) \end{aligned}$$

Then by substituting (16.17) in (16.16), I get the UK weights as

$$(16.18) \quad w_{\text{UK}} = \Gamma^{-1} \left(\gamma_0 - \Psi (\Psi^\top \Gamma^{-1} \Psi)^{-1} (\Psi^\top \Gamma^{-1} \gamma_0 - \Psi_0^\top) \right)$$

Note 162. Then by substituting 16.18 in (16.3) , the UK predictor $Z_{\text{UK}}(s_0)$ at s_0 is

$$(16.19) \quad Z_{\text{UK}}(s_0) = \left(\gamma_0 - \Psi (\Psi^\top \Gamma^{-1} \Psi)^{-1} (\Psi^\top \Gamma^{-1} \gamma_0 - \Psi_0^\top) \right)^\top \Gamma^{-1} Z$$

and by substituting 16.18 in (16.14) its standard error is

$$(16.20) \quad \sigma_{\text{UK}}(s_0) = \sqrt{-w_{\text{UK}}^\top \Gamma w_{\text{UK}} + 2w_{\text{UK}}^\top \gamma_0}$$

$$(16.21) \quad = \sqrt{\gamma_0^\top \Gamma^{-1} \gamma_0 - (\Psi^\top \Gamma^{-1} \gamma_0 - \Psi_0^\top)^\top (\Psi^\top \Gamma^{-1} \Psi)^{-1} (\Psi^\top \Gamma^{-1} \gamma_0 - \Psi_0^\top)}$$

Note 163. $(1 - \alpha)$ 100% Prediction interval of UK predictor $Z_{\text{UK}}(s_0)$ at s_0 is

$$(16.22) \quad \left(Z_{\text{UK}}(s_0) - q_{\alpha/2} \sqrt{\sigma_{\text{UK}}^2(s_0)}, Z_{\text{UK}}(s_0) + q_{1-\alpha/2} \sqrt{\sigma_{\text{UK}}^2(s_0)} \right)$$

where q_\cdot are suitable quantiles of the distribution of $Z(\cdot)$. E.g. if $Z(\cdot) \sim \text{GP}(\mu(\cdot), c(\cdot, \cdot))$ then $q_{0.05/2} = -1.96$ and $q_{0.95/2} = 1.96$ at $\alpha = 0.05$.

Note 164. Note that we have not assumed a particular distribution of $Z(\cdot)$ or $\delta(\cdot)$, but only stationarity assumptions.

Note 165. Assumption in (16.7) restricts the available models (16.2) under consideration. Essentially, it addresses the non-determination issue caused by the assumption (16.12) (introducing intrinsic stationarity δ) which can only partially characterize the covariance function of δ . Also it ensures conditional negative definiteness for 16.14.

Note 166. It was not necessary to consider the intrinsic stationarity in Note 158 to derive Universal Kriging predictor equations; formulas (16.19) & (16.20) could have been derived with respect to the covariance function $c(\cdot, \cdot)$ of $(\delta(\cdot))$ instead of its semivariogram $\gamma(\cdot)$. Here, intrinsic stationarity was assumed for practical reasons; it allowed us to express 16.19 and (16.20) as functions of the semivariogram whose estimation has been discussed in Section 15.

Note 167. Practical use of (16.19), (16.20), and (16.22) requires knowledge of the linear drift coefficients $\{\beta_j\}$ and the semivariogram $\gamma(\cdot)$. If $\{\beta_j\}$ and $\gamma(\cdot)$ are unknown, a way to learn them, is as follows. Consider a separate dataset training dataset $\{(s'_i, Z'_i)\}_{i=1}^{n'}$ (although in practice we use the same $\{(s_i, Z_i)\}_{i=1}^n$). Model the semivariogram $\gamma(\cdot)$ with a conditional negative semi-definite function $\gamma_\theta(\cdot)$ parameterized by an unknown parameter θ . Then train/estimate $\{\beta_j\}$ and $\gamma_\theta(\cdot)$ against dateset $\{(s'_i, Z'_i)\}_{i=1}^{n'}$ by using the semi-parametric procedure in Note 143 or Note 146, and plug the estimates in (16.19), (16.20), and (16.22).

Note 168. The dataset $\{(s'_i, Z'_i)\}_{i=1}^{n'}$ used to train $\{\beta_j\}$ and $\gamma(\cdot)$ should be different than the dataset $\{(s_i, Z_i)\}_{i=1}^n$ used to produce the Kriging predictive equations (16.19), (16.20), and (16.22). This is because in theory the same dataset should not be used twice (it leads to overconfidence). However often in practice the same dataset is use in violation of the theory because usually this has a small impact in the results.

Example 169.² Consider the example with the Meuse dataset. Fig 16.2b presents the UK prediction $Z_{\text{UK}}(s_0)$ at any point $s_0 \in \mathcal{S}$ under model (16.1) for which the deterministic drift mean has a linear form $\mu(s) = \beta_0 + \beta_1 s_1 + \beta_2 s_2$. Following Notes 167 and 143, we computed the $\hat{\beta}_{\text{LSE}}$ of β by (15.7), we computed the residual process $\{\hat{\delta}_i\}$ by removing the linear trend by (15.8), we computed the non-parametric estimate of semivariogram $\hat{\gamma}$ (15.2) of δ as in Proposition 125. We considered a (parametric) isotropic exponential semivariogram $\gamma_{(\sigma^2, \phi)}$ of δ where we computed the OLS $\hat{\theta}_{\text{OLS}} = (\hat{\sigma}_{\text{OLS}}^2, \hat{\phi}_{\text{OLS}})$ of the hyperparameters (σ^2, ϕ) as in (15.6) (see Figure 15.3d). Then we plugged in the estimated $\gamma_{(\hat{\sigma}_{\text{OLS}}^2, \hat{\phi}_{\text{OLS}})}$ in (16.19) to compute the UK weights w_{UK} for the UK predictor $Z_{\text{UK}}(s_0) = w_{\text{UK}}Z$ for any $s_0 \in \mathcal{S}$.

Example 170. (Cont. Examples 115, 132) Consider the example with the Meuse dataset. The dataset has another measurement (a potential regressor in the deterministic mean $\mu(s)$), the “distance to the Meuse river bed” $\{d_i\}$ at the associated locations $\{s_i\}$, let’s denote it by d . Figure 16.2c shows a rather linear relationship between Z and \sqrt{d} . Consider deterministic drift mean has a linear form $\mu(s, d) = \beta_0 + \beta_1 \sqrt{d(s)}$ while the rest specification is the same

²https://github.com/georgios-stats/Spatio-Temporal_Statistics_Michaelmas_2024/blob/main/Lecture_notes/R_scripts/03.Geostatistical_data_meuse_gstats.R

as in Example 169. We follow the same procedure as in Example 169 and we get the UK predictor in Figure 16.2d.

16.2. Ordinary Kriging.

Note 171. Ordinary Kriging (OK) addresses spatial prediction in cases that the specified statistical model on $(Z(s); s \in \mathcal{S})$ has the form

$$(16.23) \quad Z(s) = \beta_0 + \delta(s)$$

with unknown $\beta_0 \neq 0$ and intrinsically stationary process $(\delta(s); s \in \mathcal{S})$.

Note 172. OK can be derived as a special case of the Universal Kriging by setting $p = 0$ and constant spatial mean $\mu(s) = \beta_0$.

Example 173. [The derivation is in (Exercise 17 Exercise sheet).] For demonstration, we mention some key equations of OK

$$(16.24) \quad \mathfrak{L}(w, \lambda) = \underbrace{-w^\top \Gamma w + 2w^\top \gamma_0 - \lambda}_{=\text{MSE}(Z_{\text{OK}}(s_0))} \underbrace{(w^\top \underline{1} - 1)}_{\text{Assumption } \sum_{i=1}^n w_i = 1}$$

The OK system of equations is $0 = \nabla_{(\{w_i\}, \lambda)} L(w, \lambda)|_{(w, \lambda)}$ producing

$$(16.25) \quad \begin{cases} 0 = -2\Gamma w_{\text{OK}} + 2\gamma_0 - 1\lambda \\ w_{\text{OK}}^\top \underline{1} = 1 \end{cases}$$

the weights are

$$(16.26) \quad w_{\text{OK}} = \Gamma^{-1} \left(\gamma_0 + \frac{\underline{1}^\top \Gamma^{-1} \gamma_0}{\underline{1}^\top \Gamma^{-1} \underline{1}} \underline{1} \right)$$

the Kriging standard error of $Z_{\text{OK}}(s_0)$ at s_0 is

$$(16.27) \quad \sigma_{\text{OK}}^2(s_0) = \gamma_0^\top \Gamma^{-1} \gamma_0 - \frac{(\underline{1}^\top \Gamma^{-1} \gamma_0)^2}{\underline{1}^\top \Gamma^{-1} \underline{1}}.$$

Example 174. (Cont. Examples 115, 132, 170) Consider the example with the Meuse dataset. with $\mu(s) = \beta_0 + \beta_1 s_1 + \beta_2 s_2$. We do not see much difference between OK in Figure 16.2a and UK in Figure 16.2b possibly because the slopes in the linear trend (mean) of UK are rather small and insignificant (See Example 145).

16.3. Simple Kriging.

Note 175. Simple Kriging (SK) addresses spatial prediction in cases that the specified statistical model on $(Z(s); s \in \mathcal{S})$ has the form

$$(16.28) \quad Z(s) = \mu(s) + \delta(s)$$

where the deterministic mean $\mu(s)$ is known, and $(\delta(s); s \in \mathcal{S})$ is a weakly stationary process with covariogram $c(\cdot)$.

Example 176. [The derivation is in (Exercise 15 in the Exercise sheet).] It does not require any assumption in the weights such as (16.5) or (16.25). As a supplementary and for demonstration, we mention the SK predictor at s_0 and standard error:

$$Z_{\text{SK}}(s_0) = \mu(s_0) + C_0^\top C^{-1} [Z - \mu]$$

$$\sigma_{\text{SK}} = \sqrt{c(s_0, s_0) - C_0^\top C^{-1} C_0}$$

with $\mu = (\mu(s_1), \dots, \mu(s_n))^\top$, $C_0 = (c(s_0 - s_i), \dots, c(s_0 - s_n))^\top$, and $[C]_{i,j} = c(s_i - s_j)$.

Example 177. Consider the example with the Meuse dataset. Fig 16.2a presents the OK prediction $Z_{\text{OK}}(s_0)$ at any point $s_0 \in \mathcal{S}$ under model (16.23) that is the UK case (16.1) for when $\mu(s) = \beta_0$. First we computed the non-parametric semivariogram $\hat{\gamma}$ (15.2) as in Proposition 125; then we considered a (parametric) isotropic exponential semi-variogram $\gamma_{(\sigma^2, \phi)}$ where we computed the OLS $\hat{\theta}_{\text{OLS}} = (\hat{\sigma}_{\text{OLS}}^2, \hat{\phi}_{\text{OLS}})$ of the hyperparameters (σ^2, ϕ) as in (15.6) (see Figure 15.3a); and then we plugged in the estimated $\gamma_{(\hat{\sigma}_{\text{OLS}}^2, \hat{\phi}_{\text{OLS}})}$ in (16.26) to compute the OK weights w_{OK} for the OK predictor $Z_{\text{OK}}(s_0) = w_{\text{OK}} Z$ for any $s_0 \in \mathcal{S}$.

17. THE BAYESIAN KRIGING PARADIGM (HIERARCHICAL MODELING)

17.1. General framework.

Note 178. The Bayesian framework provides an elegant solution for taking into account the uncertainty on variogram or covariance parameters.

Note 179. Consider the geostatistical model for $(Z(s); s \in \mathcal{S})$ with a scale decomposition such as in (14.3)

$$(17.1) \quad Z(s) = \underbrace{\mu(s) + w(s)}_{=Y(s)} + \varepsilon(s), \quad s \in \mathcal{S}$$

where, $\mu(s) = E(Z(s))$ is an unknown drift function modelling large scale variations, $(w(s); s \in \mathcal{S})$ is a zero mean random field modelling lower scale variation, and $(\varepsilon(s); s \in \mathcal{S})$ is a nugget random field modeling measurement errors. Also $Y(s) = \mu(s) + w(s)$.

Note 180. Consider a dataset $\{(s_i, Z_i)\}_{i=1}^n$ with $Z_i = Z(s_i)$ being a realization of (17.1) at site $s_i \in \mathcal{S}$.

Note 181. Unlike in the traditional kriging framework, in Bayesian kriging, we have to specify a certain probabilistic model on the spatial random fields. Uncertainty can be decomposed

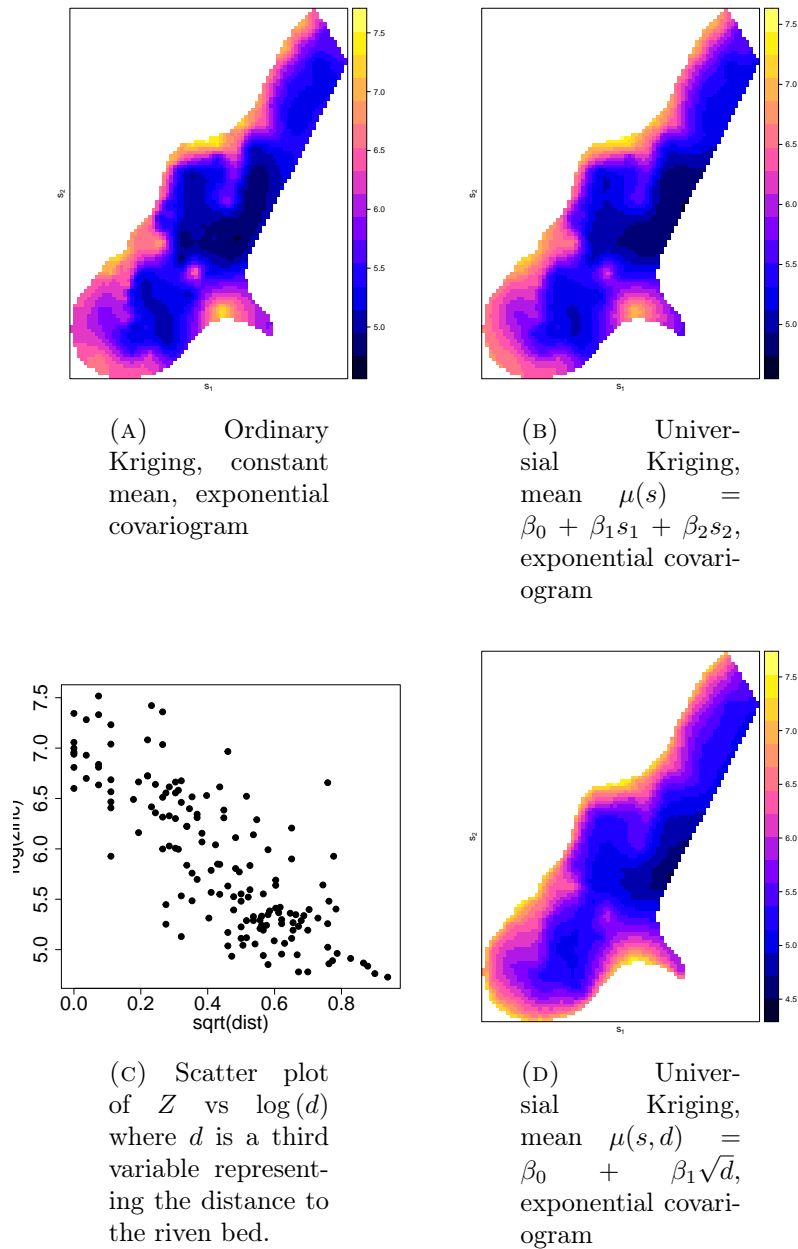


FIGURE 16.2. Kriging Meuse dataset.

according to the Hierarchical spatial model

$$(17.2) \quad \begin{cases} Z|Y, \theta_1, \theta_2 & \text{data model} \\ Y|\theta_1, \theta_2 & \text{spatial process model} \\ \theta_1 & \text{hyper-priormodel (optional layer)} \end{cases}$$

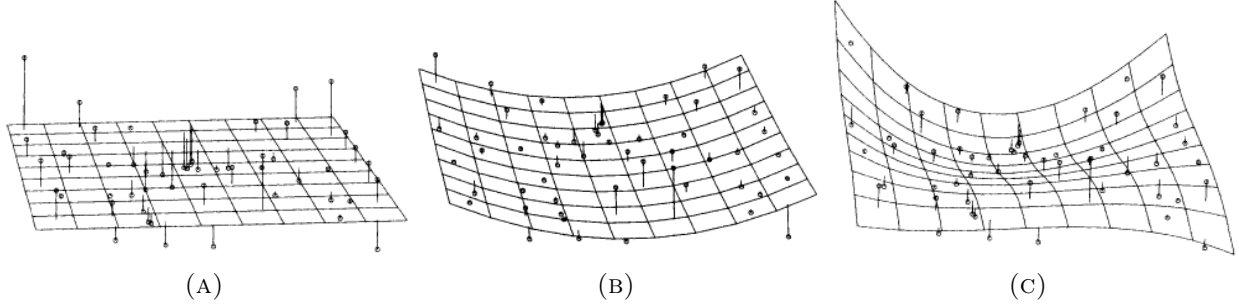


FIGURE 17.1. Examples representing the hierarchical spatial model 17.2 for different values of ϑ

with

$$\text{pr}(Z, Y, \theta_1 | \theta_2) = \text{pr}(Z|Y, \theta_1, \theta_2) \text{pr}(Y|\theta_1, \theta_2) \text{pr}(\theta_1|\theta_2)$$

where $Z = (Z_1, \dots, Z_n)^\top$, $Y = (Y_1, \dots, Y_n)^\top$, with $Y_i = Y(s_i)$. Here, $\theta_1 \in \Theta_1$ is an unknown random hyper parameter following prior $\theta_1|\theta_2 \sim \text{pr}(\theta_1|\theta_2)$, and $\theta_2 \in \Theta_2$ is an unknown fixed parameter without a specified prior.

Note 182. Spatial process model expresses the scientific uncertainty (e.g., that coming from $(Y(\cdot))$) as quantified via the specified distribution $\text{pr}(Y|\theta)$ possibly labeled by some hyper-parameter $\theta = (\theta_1, \theta_2)^\top$. Data model expresses the measurement uncertainty (e.g., that coming from $(\varepsilon(\cdot))$) as quantified via the distribution $\text{pr}(Z|Y, \theta)$ possibly labeled by some parameter θ .

Note 183. Figure 17.1 presents a visualization of the hierarchical model in Notes 181. The surfaces can be considered as a realization of the spatial process model $Y(\cdot)$, and the dots can be considered as realizations of the data model $\varepsilon(\cdot)$ at specific sites given the spatial process.

Note 184. Under Bayesian model (17.2), unknown but fixed θ_2 can be learned pointwise by computing a point estimator $\hat{\theta}_2$ via marginal likelihood maximization

$$\hat{\theta}_2 = \arg \min_{\theta_2} (-2 \log (\text{pr}(Z|\theta_2))),$$

where $\text{pr}(Z|\theta_2) = \int \text{pr}(Z, Y, \theta_1 | \theta_2) dY d\theta_1$

Note 185. Under Bayesian model (7.2), uncertainty about unknown random θ_1 can be represented by the posterior distribution

$$\text{pr}(\theta_1 | Z, \theta_2 = \hat{\theta}_2) = \frac{\text{pr}(Z|\theta_1, \theta_2 = \hat{\theta}_2) \text{pr}(\theta_1|\theta_2 = \hat{\theta}_2)}{\text{pr}(Z|\theta_2 = \hat{\theta}_2)}$$

where the value $\hat{\theta}_2$ is plugged in.

Note 186. The posterior predictive distributions of the spatial process model ($Y(\cdot)$) given the data Z is

$$(17.3) \quad \text{pr} \left(Y(s_0) | Z, \theta_2 = \hat{\theta}_2 \right) = \int \text{pr} \left(Y(s_0) | Z, \theta_1, \theta_2 = \hat{\theta}_2 \right) \text{pr} \left(\theta_1 | Z, \theta_2 = \hat{\theta}_2 \right) d\theta_1$$

and the marginal process ($Z(\cdot)$) given the data Z is

$$(17.4) \quad \text{pr} \left(Z(s_0) | Z, \theta_2 = \hat{\theta}_2 \right) = \int \text{pr} \left(Z(s_0) | Z, \theta_1, \theta_2 = \hat{\theta}_2 \right) \text{pr} \left(\theta_1 | Z, \theta_2 = \hat{\theta}_2 \right) d\theta_1$$

for any $s_0 \in \mathcal{S}$.

Note 187. The Bayes Kriging predictor $\hat{Y}_{\text{BK}}(s_0)$ of $Y(s_0)$ at unseen location s_0 equations is the optimizer

$$(17.5) \quad \hat{Y}_{\text{BK}}(s_0) = \arg \min_{Y_{\text{BK}}(s_0)} (\text{E}(\ell(Y_{\text{BK}}(s_0), Y(s_0)) | Z))$$

given a pre-specified loss function $\ell : \mathcal{Z} \times \mathcal{Z} \rightarrow \mathbb{R}_+$. The expectation is under the probability (17.4). For Bayes Kriging predictor $\hat{Z}_{\text{BK}}(s_0)$ of $Z(s_0)$ at s_0 is

$$(17.6) \quad \hat{Z}_{\text{BK}}(s_0) = \arg \min_{Z_{\text{BK}}(s_0)} (\text{E}(\ell(Z_{\text{BK}}(s_0), Z(s_0)) | Z))$$

17.2. An example: Gaussian process regression.

Note 188. We are going through a particular example of the Bayesian Kriging (or Bayesian Gaussian process regression) to demonstrate how the “Bayesian Kriging” works.

List of useful formulas.

Fact 189. Let $X \sim N(\mu_X, \Sigma_X)$, $Y \sim N(\mu_Y, \Sigma_Y)$ and Y, X independent. Let fixed matrices A and B and vector c of appropriate sizes. Then

$$(17.7) \quad AX + BY + c \sim N(A\mu_X + B\mu_Y + c, A\Sigma_X A^\top + B\Sigma_Y B^\top)$$

Fact 190. Let $N(\beta|b, B)$ be the Gaussian pdf with mean b and covariance B at β . It is

$$\int N(Z|\Psi\beta, C) N(\beta|b, B) d\beta = N(Z|\Psi b, C + \Psi B \Psi^\top)$$

Fact 191. (Woodbury matrix identity) It is

$$(A + BCD)^{-1} = A^{-1} - A^{-1}B(C^{-1} + DA^{-1}B)^{-1}DA^{-1}$$

Fact 192. [Marginalization & conditioning] Let $x_1 \in \mathbb{R}^{d_1}$, and $x_2 \in \mathbb{R}^{d_2}$. If

$$\begin{bmatrix} x_1 \\ x_2 \end{bmatrix} \sim N_{d_1+d_2} \left(\begin{bmatrix} \mu_1 \\ \mu_2 \end{bmatrix}, \begin{bmatrix} \Sigma_1 & \Sigma_{21}^\top \\ \Sigma_{21} & \Sigma_2 \end{bmatrix} \right)$$

then it is

$$x_2|x_1 \sim N_{d_2}(\mu_{2|1}, \Sigma_{2|1})$$

where

$$\mu_{2|1} = \mu_2 + \Sigma_{21}\Sigma_1^{-1}(x_1 - \mu_1) \quad \text{and} \quad \Sigma_{2|1} = \Sigma_2 - \Sigma_{21}\Sigma_1^{-1}\Sigma_{21}^\top$$

Note 193. Consider an available dataset $\{(s_i, Z_i)\}_{i=1}^n$ with $\{Z_i \in \mathbb{R}\}$ and $\{s_i \in \mathcal{S}\}$. The i -th datum $Z_i = Z(s_i)$ may be an independent measurement of an unobserved quantity $Y_i = Y(s_i)$ at location s_i but contaminated by additive random error $\varepsilon_i = \varepsilon(s_i)$; i.e. $Z_i = Y_i + \varepsilon_i$ for $i = 1, \dots, n$. Interest lies in recovering functions $Z(\cdot)$ and/or $Y(\cdot)$ over the spatial domain \mathcal{S} .

Specifying the hierarchical model.

Note 194. The geostatistical model can be considered as

$$(17.8) \quad Z(s) = \underbrace{\mu(s) + w(s)}_{=Y(s)} + \varepsilon(s), \quad s \in \mathcal{S}$$

$\mu(\cdot)$: is a deterministic systematic drift $\mu(s) = E(Z(s))$ modeling large scale variation;
 $w(\cdot)$: models smaller scale variation, it is modeled as a Gaussian process

$$w(\cdot) \sim GP(0, c(\cdot, \cdot))$$

with covariance function $c : \mathcal{S} \times \mathcal{S} \rightarrow \mathbb{R}$ and mean function zero.

$\varepsilon(\cdot)$: models the additive random measurement error, it is modeled as a Gaussian process

$$\varepsilon(\cdot) \sim \text{GP}(0, c_{\text{nugget}}(\cdot, \cdot | \sigma^2))$$

with nugget covariance function $c_{\text{nugget}}(s, s' | \sigma^2) = \sigma^2 \mathbf{1}_{\{0\}}(|s - s'|)$.

Assuming, $w(\cdot) \perp \varepsilon(\cdot)$, it is implied

$Y(\cdot)$: models the noisiness signal

$$Y(\cdot) \sim \text{GP}(\mu(\cdot), c(\cdot, \cdot))$$

$Z(\cdot)$: is the marginal process

$$Z(\cdot) \sim \text{GP}(\mu(\cdot), c_Z(\cdot, \cdot))$$

where $c_Z(s, s') = c(s, s') + \sigma^2 \mathbf{1}_{\{0\}}(|s - s'|)$ assuming that $w(\cdot)$ and $\varepsilon(\cdot)$ are independent.

Note 195. The resulted hierarchical model is

$$(17.9) \quad \begin{cases} Z|Y \sim \mathcal{N}(Y, I\sigma^2) & \text{data model} \\ Y \sim \mathcal{N}(\mu(S), C(S, S)) & \text{spatial process model} \end{cases}$$

where $[Z]_i = Z(s_i)$, $[Y]_i = Y(s_i)$, $[\mu(S)]_i = \mu(s_i)$, and $[C(S, S)]_{i,j} = c(s_i, s_j)$.

The predictive distribution of $Y(\cdot)|Z$ under (17.9).

Note 196. Assume a vector of “unseen” sites $S_* = (s_{*,1}, \dots, s_{*,q})^\top$ for any $q \in \mathbb{N}_0$. The joint marginal distribution of $(Y_*, Z)^\top$ where $Z := Z(S)$ and $Y_* := Y(S_*)$ is

$$(17.10) \quad \begin{pmatrix} Y_* \\ Z \end{pmatrix} \sim \mathcal{N}\left(\begin{pmatrix} \mu(S_*) \\ \mu(S) \end{pmatrix}, \begin{pmatrix} C(S_*, S_*) & (C(S_*, S))^\top \\ C(S_*, S) & C(S, S) + I\sigma^2 \end{pmatrix}\right)$$

by using convenient notation $[C(S_*, S)]_{i,j} = c(s_{*,i}, s_j)$ and $[\mu(S)]_i = \mu(s_i)$.

Note 197. The (posterior) predictive distribution of $Z_*|Z$ is the conditional distribution

$$(17.11) \quad Y_*|Z \sim \mathcal{N}(\mu_1(S_*), C_1(S_*, S_*))$$

where

$$(17.12) \quad C_1(S_*, S_*) = C(S_*, S_*) + (C(S, S_*))^\top (C(S, S) + I\sigma^2)^{-1} C(S, S_*)$$

$$(17.13) \quad \mu_1(S_*) = \mu(S_*) - (C(S, S_*))^\top (C(S, S) + I\sigma^2)^{-1} (\mu(S) - Z)$$

[We used Fact 192].

Note 198. Since derivation of (17.11) holds for all vectors $S_* \in \mathbb{R}^q$ and all $q > 0$, (17.11) can be extended to a Gaussian Process

$$(17.14) \quad Y(\cdot) | Z \sim \text{GP}(\mu_1(\cdot), c_1(\cdot, \cdot))$$

with

$$\begin{aligned} c_1(s, s') &= c(s, s') + (C(S, s))^T (C(S, S) + I\sigma^2)^{-1} C(S, s') \\ \mu_1(s) &= \mu(s) - (C(S, s))^T (C(S, S) + I\sigma^2)^{-1} (\mu(S) - Z) \end{aligned}$$

for any $s, s' \in \mathcal{S}$. This is the predictive process for noiseless signal $Y(s)$ at any $s \in \mathcal{S}$ given Z . [Here we used the definition of GP (Definition 17) given Note 196].

The predictive distribution of $Z(\cdot) | Z$ under (17.9).

Note 199. It is a Gaussian Process

$$(17.15) \quad Z(\cdot) | Z \sim \text{GP}(\mu_1(\cdot), c_1^z(\cdot, \cdot))$$

with $c_1^z(s, s') = c_1(s, s') + \sigma^2 1_{\{0\}}(|s - s'|)$. This is because $Z(\cdot) = Y(\cdot) + \varepsilon(\cdot)$ with $Y(\cdot) \perp \varepsilon(\cdot)$.

Learning $\mu(\cdot)$ and $c(\cdot, \cdot)$ via parametrization.

Note 200. Let $\mu(\cdot)$ be parametrised as $\mu(s|\beta) = \psi(s)^\top \beta$ with known basis functions $\psi(\cdot) = (\psi_1(\cdot), \dots, \psi_p(\cdot))^\top$, and unknown random parameter $\beta \in \mathbb{R}^p$ following prior distribution $\beta \sim N(b, B)$, $B > 0$. Let $c(\cdot, \cdot|\theta)$ be parametrised as $c(\cdot, \cdot) = c(\cdot, \cdot|\theta)$ with unknown fixed parameter $\theta \in \Theta$. Let σ^2 be an unknown fixed parameter.

Note 201. The Bayesian hierarchical model summaries to

$$(17.16) \quad \begin{cases} Z|Y, \sigma^2 \sim N(Y, I\sigma^2) & \text{data model} \\ Y|\beta, \theta \sim N(\mu(S), c(S, S)) & \text{spatial process model} \\ \beta \sim N(b, B) & \text{hyper-prior model} \end{cases}$$

Note 202. The posterior of β given data Z and θ is computed via the Bayes theorem

$$\begin{aligned} \text{pr}(\beta|Z, \theta, \sigma^2) &\propto \text{pr}(Z|\beta, \theta, \sigma^2) \text{pr}(\beta) \\ &\propto N(Z|\Psi\beta, C(S, S|\theta) + I\sigma^2) N(\beta|b, B) \end{aligned}$$

and results as

$$(17.17) \quad \beta|Z, \theta, \sigma^2 \sim N(b_n(\theta, \sigma^2), B_n(\theta, \sigma^2))$$

with

$$B_n(\theta, \sigma^2) = \left(B^{-1} + \Psi^\top (C(S, S|\theta) + I\sigma^2)^{-1} \Psi \right)^{-1}$$

$$b_n(\theta, \sigma^2) = B_n(\theta, \sigma^2) \left(B^{-1} b + \Psi^\top (C(S, S|\theta) + I\sigma^2)^{-1} Z \right)$$

[For the calculations of the derivation see Exercise 18 in the Exercise sheet.]

Note 203. Given a vector of “unseen” sites $S_* = (s_{*,1}, \dots, s_{*,q})^\top$ for any $q \in \mathbb{N}_0$, I integrate 17.11 with respect to (17.17) i.e.

$$\begin{aligned} \text{pr}(Y_*|Z, \theta, \sigma^2) &= \int \text{pr}(Y_*|Z, \beta, \theta, \sigma^2) \text{pr}(\beta|Z, \theta, \sigma^2) d\beta \\ &= \int N(Y_*|\mu_1(S_*|\beta, \theta, \sigma^2), C_1(S_*, S_*|\theta, \sigma^2)) N(\beta|b_n(\theta, \sigma^2), B_n(\theta, \sigma^2)) d\beta \end{aligned}$$

where now $C(|\theta, \sigma^2)$, $C_1(|\theta, \sigma^2)$ and $\mu_1(|\theta, \sigma^2, \beta)$ are parameterized by β , θ , and σ^2 . By using Fact 190

$$(17.18) \quad Y_*|Z, \theta, \sigma^2 \sim N(\mu_2(S_*|\theta, \sigma^2), C_2(S_*, S_*|\theta, \sigma^2))$$

where

$$(17.19)$$

$$\begin{aligned} C_2(S_*, S_*|\theta, \sigma^2) &= C_1(S_*, S_*|\theta, \sigma^2) \\ &\quad + \left[\Psi(S_*) - (C(S, S_*|\theta))^\top (C(S, S|\theta) + I\sigma^2)^{-1} \Psi(S_*) \right] \\ &\quad \times B_n(\theta, \sigma^2) \left[\Psi(S_*) - (C(S, S_*|\theta))^\top (C(S, S|\theta) + I\sigma^2)^{-1} \Psi(S_*) \right]^\top \\ (17.20) \quad \mu_2(S_*|\theta, \sigma^2) &= \Psi(S_*) b_n(\theta, \sigma^2) - (C(S, S_*|\theta))^\top (C(S, S|\theta) + I\sigma^2)^{-1} (\Psi(S) b_n(\theta, \sigma^2) - Z) \end{aligned}$$

Note 204. Since derivation of (17.18) holds for all vectors $S_* \in \mathbb{R}^q$ and all $q > 0$, (17.18) can be extended to a Gaussian Process

$$(17.21) \quad Y(\cdot)|Z, \theta, \sigma^2 \sim GP(\mu_2(\cdot|\theta, \sigma^2), c_2(\cdot, \cdot|\theta, \sigma^2))$$

$$(17.22)$$

$$\begin{aligned} \mu_2(s|\theta, \sigma^2) &= \psi(s) b_n(\theta, \sigma^2) - (C(s|\theta))^\top (C(\theta) + I\sigma^2)^{-1} (\Psi b_n(\theta, \sigma^2) - Z) \\ (17.23) \quad c_2(s, s'|\theta, \sigma^2) &= c_1(s, s'|\theta, \sigma^2) \\ &\quad + \left[\psi(s) - (C(s|\theta))^\top (C(\theta) + I\sigma^2)^{-1} \Psi \right] B_n(\theta, \sigma^2) \left[\psi(s) - (C(s|\theta))^\top (C(\theta) + I\sigma^2)^{-1} \Psi \right] \end{aligned}$$

with column vector $C(s|\theta) = (c(s, s_1), \dots, c(s, s_n))^\top$, and matrix $C(\theta) := C(S, S|\theta)$.

Note 205. Estimates $\hat{\theta}$ and $\hat{\sigma}^2$ of the unknown fixed hyper-parameters θ and σ^2 are computed by maximizing the marginal likelihood of Z given θ and σ^2

$$(17.24) \quad \text{pr}(Z|\theta, \sigma^2) = \int \text{pr}(Z|\beta, \theta, \sigma^2) \text{pr}(\beta) d\beta$$

$$(17.25) \quad = \int N(Z|\Psi\beta, C(\theta) + I\sigma^2) N(\beta|b, B) d\beta$$

$$(17.26) \quad = N(Z|\Psi b, C(\theta) + I\sigma^2 + \Psi B \Psi^\top)$$

where $C(\theta) := C(S, S|\theta)$ [from Fact 190] by computing

$$\left(\hat{\theta}, \hat{\sigma}^2 \right) = \arg \min_{\theta, \sigma^2} \left(-2 \log \left(N(Z|\Psi b, C(\theta) + I\sigma^2 + \Psi B \Psi^\top) \right) \right)$$

The predictive distribution of $Z(\cdot)|Z$ after parameterization.

Note 206. It is a Gaussian Process

$$(17.27) \quad Z(\cdot)|Z, \theta, \sigma^2 \sim GP\left(\mu_2(\cdot|\theta, \sigma^2), c_2^z(\cdot, \cdot|\theta, \sigma^2)\right)$$

with $c_2^z(s, s'|\theta, \sigma^2) = c_2(s, s'|\theta, \sigma^2) + \sigma^2 1_{\{0\}}(|s - s'|)$. This is because $Z(\cdot) = Y(\cdot) + \varepsilon(\cdot)$ with $Y(\cdot) \perp \varepsilon(\cdot)$.

Note 207. The estimated ‘‘Kriging predictor’’ results by plugging $\hat{\theta}$ and $\hat{\sigma}^2$ in (17.21)

$$(17.28) \quad Y(\cdot)|Z, \hat{\theta}, \hat{\sigma}^2 \sim GP\left(\mu_2(\cdot|\hat{\theta}, \hat{\sigma}^2), c_2(\cdot, \cdot|\hat{\theta}, \hat{\sigma}^2)\right)$$